Applied Energy 314 (2022) 118957

Contents lists available at ScienceDirect

Applied Energy

journal homepage: www.elsevier.com/locate/apenergy

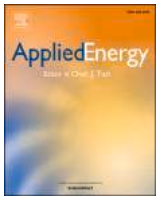

Energetic and thermal comfort assessment of phase change material passively incorporated building envelope in severe hot Climate: An experimental study

Qudama Al-Yasiri [a,b,c,*], Márta Szabó [b]

[a] Doctoral School of Mechanical Engineering, Hungarian University of Agriculture and Life Sciences, Szent István campus, Páter K. u. 1, Gödöllő H-2100, Hungary
[b] Department of Building Engineering and Energetics, Institute of Technology, Hungarian University of Agriculture and Life Sciences, Szent István campus, Páter K. u. 1, Gödöllő H-2100, Hungary
[c] Department of Mechanical Engineering, Faculty of Engineering, University of Misan, Al Amarah City, Misan Province 62001, Iraq

HIGHLIGHTS

- A PCM macroencapsulated panel and capsules is incorporated into building envelope under severe hot climate.
- The optimal PCM position and thickness in the roof and the best thermally-performed PCM bricks are considered.
- The MTR, ATFR, DF, TL, OTD and DHR are calculated.
- The roof and east wall are performed better, especially under high outdoor temperatures.
- The PCM is not efficient to maintain suitable thermal comfort when incorporated passively.

ARTICLE INFO

Keywords:
PCM
Building energy-saving
Thermal comfort
Thermal performance
Peak temperature reduction
Building envelope

ABSTRACT

Phase change materials (PCMs) can beneficially work as a successful thermal energy storage medium in different applications. PCMs have shown a remarkable enhancement in building energy-saving and thermal comfort in hot locations. In this paper, the thermal behaviour of a PCM-enhanced thermally-poor building envelope is studied experimentally. To this aim, two identical rooms, one loaded with PCM (PCM room) and the other without (reference room), are built and tested under a severe hot climate of Al Amarah city, Iraq. Previously examined parameters, such as the optimal position and thickness of the PCM layer in the roof and the best-thermally performed PCM capsules integrated concrete bricks, are considered to build the PCM room. Several energetic and thermal comfort indicators such as maximum temperature reduction (MTR), average temperature fluctuation reduction (ATFR), decrement factor (DF), time lag (TL), operative temperature difference (OTD), discomfort hours reduction (DHR) and maximum heat gain reduction (MHGR) are determined and discussed to show the potential of PCM. The experimental results revealed that the incorporated PCM could remarkably improve the thermal performance of building envelope exposed to high outdoor temperatures. Amongst envelope elements and compared with the reference room, the roof and east wall of the PCM room recorded the best thermal behaviour, where the MTR difference, ATFR, DF, and TL difference reached 3.75 °C, 6.5 °C, 25.6%, 70 min for the roof, and 2.75 °C, 2.4 °C, 12.8% and 40 min for the east wall, respectively. Moreover, the PCM room shows a thermal comfort enhancement by 11.2% and 34.8%, considering the DHR and MHGR, respectively, compared with the reference one. The study highlighted that suitable ventilation means are necessary to improve the building performance and reach acceptable thermal comfort when the PCM is incorporated passively.

1. Introduction

Buildings are the major consumer of global final energy use by a ratio

* Corresponding author at: Doctoral School of Mechanical Engineering, Hungarian University of Agriculture and Life Sciences, Szent István campus, Páter K. u. 1, Gödöllő H-2100, Hungary.
E-mail address: qudamaalyasiri@uomisan.edu.iq (Q. Al-Yasiri).

https://doi.org/10.1016/j.apenergy.2022.118957
Received 24 November 2021; Received in revised form 30 January 2022; Accepted 13 March 2022

Nomenclature

Abbreviations

ATFR	Average temperature fluctuation reduction [°C]
CLR	Cooling load reduction [%]
DF	Decrement factor [unitless]
DHR	Discomfort hours reduction [%]
DSC	Differential scanning calorimeter
HG	Heat gain (W)
HTR	Heat transfer reduction [%]
ITR	Indoor temperature reduction [°C]
MHGR	Maximum heat gain reduction [%]
MTR	Maximum temperature reduction [°C]
OT	Operative temperature [°C]
OTD	Operative temperature difference [°C]
PCM	Phase change material
TL	Time lag [min]
X	Average decrease of room temperature in the day [°C]
Y	Average increase of room temperature in the night [°C]

Symbols

A	Area [m^2]
h_i	Combined convective and radiative heat transfer coefficient for the interior element surface and interior room temperature [$W/m^2.K$]
HG_{PCM}	Heat gain of the PCM room [W]
$HG_{ref.}$	Heat gain of the reference room [W]
$OT_{PCM\ room}$	Operative temperature of the PCM room [°C]
$OT_{ref.\ room}$	Operative temperature of the reference room [°C]
SR	Solar radiation [W/m^2]
T_a	Indoor ambient temperature [°C]
T_{amb}	Outdoor ambient temperature [°C]
$T_{av.,PCM}$	Average temperature of the element of the PCM room [°C]
$T_{av.,ref.}$	Average temperature of the element of the reference room [°C]
T_i	Inside element surface temperature [°C]
T_r	Interior designed air temperature [°C]
$\overline{T}_{mr}$	Mean radiant temperature [°C]
T_o	Outside element surface temperature [°C]
$T_{R,\max}$	Outdoor maximum surface temperature of the roof [°C]
$T_{R,\min}$	Outdoor minimum surface temperature of the roof [°C]
$T_{r,\max}$	Indoor maximum surface temperature of the roof [°C]
$T_{r,\min}$	Indoor minimum surface temperature of the roof [°C]
$\tau_{R,\max}$	Time at maximum exterior roof surface temperature [min]
$\tau_{r,\max}$	Time at maximum interior roof surface temperature [min]

of up to 40% [1,2]. Building envelope is the main contributor to this percentage as it is responsible for direct heating and cooling load through the building [3]. According to the International Energy Agency, applying passive systems on the building envelope is among the key global considerations set to meet net-zero carbon emissions in the building sector by 2050 [4]. Therefore, energy policymakers and responsible parties are working to improve this essential sector following different passive methods targeting the thermal mass in most cases [5–9].

Among the booming technologies nowadays, using phase change material (PCM) as a thermal energy storage medium within the building envelope has shown interesting advancements in thermal energy management. In this regard, PCMs have been used to provide heat supply or insulation for buildings under cold and hot locations, respectively [10,11]. PCMs were incorporated efficiently with building roofs [12], walls [13], concrete [14,15], mortars [16–18], bricks [19], windows [20] and insulations [21].

PCMs are typically applied passively or actively into the building envelope. Although the passive technique has economic and technical benefits, it still suffers from thermal control issues such as unrestrained heat flow and inefficient heat charging/discharging concerns [22,23]. Therefore, adopting a proper PCM integration procedure is essential considering the suitable PCM type, effective PCM position and quantity, and the efficient incorporation method [24,25]. Researchers are rarely considering all the above influential aspects, which influence the thermal performance of PCM during the service period [26].

Most literature studies investigating PCM benefits when incorporated into building envelopes are numerical against a limited number of experiments. For instance, Hamadani et al. [27] investigated the potential of PCM to decrease the energy consumption for buildings exposed to Algerian Saharan climate conditions. They used a newly developed Trnsys module to evaluate different PCMs incorporated building envelope considering the mean air temperature, daily average temperature fluctuations, monthly and annual energy-saving. Moreover, the study proposed a new integration method using movable PCM panels instead of fixed ones to improve the system performance. Simulation results showed that annual energy-saving of 50.71% and indoor temperature reduction of 2.36 °C–4 °C could be achieved with a suitable PCM integration. Triano-Ju'arez et al. [28] numerically studied concrete roof-integrated PCM with different thicknesses and positions, and coated with grey and white colours under Mexican hot weather conditions. The study indicated that the grey-coated roof had different thermal responses for each PCM thickness and position. In contrast, the white-coated roof had negligible differences with PCM thickness and position change. The grey-coated roof's maximum interior surface temperature and cooling load reduction were 6.4 °C and 22.2%. This occurred with 2 mm PCM thickness and the position when the layer was placed close to the interior environment. In comparison, the maximum reduction in the white-coated roof reached 14.7 °C–15.4 °C and 58.1%-62.7%, respectively. Wang et al. [29] numerically studied PCM wallboards applied to the exterior building walls with different orientations under Shanghai weather conditions. The building energy-saving was studied at different PCM types with a melting temperature ranging from 20 °C to 26 °C, the optimal temperature range on a seasonal basis. The results revealed that the PCM of 24 °C melting temperature is optimal for the summer period, and the east-oriented wall has the highest energy-saving rate of about 27.78%. Whereas the PCM of 22 °C melting temperature was optimal for the winter season and the south-oriented wall saved energy by up to 96.2%. Sovetova et al. [30] studied the thermal performance and energy-saving earned from thirteen different PCM types under eight desert climates using EnergyPlus software. Their study revealed that higher PCM melting temperature performed better and thicker PCM resulted in better thermal performance (and vice versa). The study exhibited building energy-saving in the range of 17.97% to 34.26% and reducing the maximum temperature by up to 2.04 °C using suitable PCM under each location. Louanate et al. [31] studied the potential of PCM incorporation into six different climate zones in Morrocco. They found that an energy-saving of about 41% can be achieved by considering the local temperature variation and PCM's position and thickness. Bimaganbetova et al. [32] numerically investigated several PCMs of melting temperature ranging from 21 °C to 31 °C for eight tropical savanna climate locations, namely Bamako in Mali, Bangkok in Thailand, Brasilia in Brazil, Dar es Salaam in Tanzania, Bangalore and Kolkata in India, Maputo in Mozambique and Surabaya in Indonesia. The study considered the best location inside a building model walls with a PCM thickness of 20 mm using DesignBuilder software. Simulation results presented the potential of PCM on a hot summer day in which the peak temperature was shaved by up to 3.28 °C. Moreover, the

temperature fluctuation reduced by up to 2.76 °C and building energy consumption decreased by 16.58%-68.63%, showing significant advantages of PCMs under studied locations. Sharma and Rai [33] investigated the PCM potential under hot weather of Delhi (capital of India), considering the effect of PCM melting temperature (from 24 °C to 50 °C), optimal thickness (from 10 to 30 mm) and position within building sturucture. Their numerical results revealed that best PCM thermal performance depends largely on the PCM thickness and position more than the PCM melting temperature. Besides, the heat gain reduced by 12.6%–36.2% and 10.4%–26.6% when PCM enhanced the roof and walls, respectively, compared with the case of non-PCM envelopes. Su et al. [34] studied the thermal performance of a building integrated binary microencapsulated PCM under Hangzhou, China weather conditions. For this purpose, Ansys Fluent and ESP-r tools were used to simulate the PCM behaviour in typical walls and analyse whether or not to meet annual thermal comfort requirements. Findings showed that increasing the binary PCM layer from 1 mm to 5 mm can increase the energy charging/discharging rate during the day and night. At this thickness, the maximum temperature was reduced by 6.7 °C and the comfort hours enlarged by 12% compared with no PCM walls. Lakhdari et al. [35] numerically examined dual PCMs mixed with plaster as cladding material for thermal improvement of buildings located at vary climate zones. Numerical findings showed that the building temperature was reduced by 2 °C with a heat reduction by up to 75% and time shifting by up to 3 h. The study emphasised that dual PCM can enhance the thermal storage of building elements and improve their performance regardless the building location.

In experimental studies, Rathore et al. [36] tested the thermal behaviour of pipe macroencapsulated PCM integrated thin cubicles under tropical weather conditions of India. The study considered several indicators to show the thermal response of the PCM cubicle against another reference cubicle without PCM. These indicators are explicitly the peak temperature reduction, thermal amplitude reduction, time lag, cooling load reduction and the equivalent energy cost saving. Results indicated that the peak temperature reduced by 7.19%−9.18%, and the thermal amplitude reduced by 0.67%−59.79% considering the roof and all walls. The results further showed that the east and north walls had a time lag of 120 min for the PCM cubicle, whereas the roof, west and south walls showed a 60 min time delay compared with the reference cubicle. The PCM cubicle also reduced the cooling load by 38.76%, equivalent to cost-saving on the electricity of 28.31 Rupees/day (~0.40US $/day). Kenzhekhanov et al. [37] numerically and experimentally investigated PCM-based buildings' thermal performance in different locations worldwide with various conditions according to Koppen-Geiger climate classification. The annual energy saving, average temperature fluctuation reduction, maximum temperature reduction and the reduction of discomfort hours were considered to evaluate the PCM performance in each location. The results indicated an annual energy-saving of about 4.000–10.000 kWh was achieved in all investigated locations using PCMs of 23 °C–24 °C melting temperature. Furthermore, a maximum temperature reduction of more than 2 °C was obtained during the summer months. At the same time, the discomfort hours were reduced annually by 500 h. Kong et al. [38] examined building walls constructed with cement mortar panels enhanced by PCM macroencapsulated tubes, spheres and flattened plate containers. The study extended numerically to show the effect of mortar panel thickness and position on the thermal response inside the building. Results revealed that the mortar-based tube and sphere PCM capsules showed the same thermal performance, whereas the plate mortar panel indicated non-uniform temperature distribution. The results further revealed that the PCM quantity and position significantly influence the thermal response of mortar. Higher PCM quantity and position close to the indoor resulted in lower indoor temperature and longer time lag. Akeiber et al. [39] conducted an experimental study to show the benefits of paraffin wax of three melting temperatures, namely 19–37 °C (PCM1), 35–40 °C (PCM2) and 40–44 °C (PCM3), incorporated room of (1 × 1 × 1.06 cm) under weather conditions of Baghdad, Iraq. The PCM was macroencapsulated inside aluminium panels with 6 cm thickness and insulated with a 30 mm fiberglass cover for insulation. The temperature fluctuation reduction, heat flux reduction and annual energy cost saving were investigated. Results indicated that PCM3 had shown suitable temperature fluctuation and good thermal performance due to its low thermal conductivity and high thermal storage capacity. Moreover, the heat flux reduced by 21.9% and 35.1% for PCM3 compared with PCM2 and PCM1, respectively.

As seen from literature studies, PCM application in the building envelope has been investigated in different regions worldwide, showing considerable advancements. However, there is still a lack of studies dealing with experimentations under severe hot climate conditions [40]. Besides, most experimental studies did not consider all influential aspects of PCM incorporation, such as the optimal PCM position, optimal thickness and the proper encapsulation method, mostly conducted numerically [41,42]. Therefore, this research aims to consider all these aspects that we investigated previously (i.e., the optimal PCM position [43], quantity [44] and the best encapsulation method [45,46]) to study the PCM thermal performance incorporated typical residential construction materials. A detailed energetic and thermal comfort assessment was conducted under a severe hot climate of Al Amarah city, southern Iraq, where the temperature often reaches 50 °C during summer days. According to the best knowledge of the authors, no similar research has been done under the conditions of this city up to date. The results of this work are believed to afford a clear vision of the PCM-enhanced envelope thermal behaviour and contribution to building energy performance under severe hot climates for further modifications and PCM performance optimisation.

2. Methodology

2.1. Experimental rooms

Two identical rooms were built with 1 m^3 size; one included PCM in the roof and walls (PCM room), whereas the other was without PCM for comparison (reference room). The materials used for rooms construction are the thermally-poorest in Iraq, resulting in high cooling loads [47]. Both rooms were placed in an open atmosphere and exposed directly to solar radiation all day long. The rooms are situated on a high-density wood plate (3 cm thickness) to ensure no thermal influence of the foundation and guarantee that the rooms' ambient temperature is influenced by the walls and roof only. Both rooms were spaced by 120 cm to avoid the shadow effect of one on the other during sun inclination. Furthermore, a small openable window with a wooden frame (25 × 35 cm) was fixed on the East wall to allow the real influence of solar radiation on the indoor environment. However, both windows were kept close all day long to investigate the thermal behaviour of PCM under a non-conditioned state. All slots of joined elements were closed using high-density foam to ensure no air infiltration between the indoor and outdoor environments. The detailed information about the construction materials used for rooms fabrication is detailed in Table 1.

Both tested rooms were oriented to the east-south direction. The final form of tested rooms is shown in Fig. 1.

2.2. Preparation of PCM panel and PCM capsules

Locally available paraffin wax was used as a PCM in this work. This PCM type is a petroleum-based product generated during the de-waxing process of the Iraqi crude oil at the Iraqi governmental refineries. It has a melting temperature in the range of 40 °C−44 °C according to the differential scanning calorimeter (DSC) test shown in Fig. 2, making it a suitable candidate for the temperature variation in the location under study and the passive technique adopted. More characteristics of this PCM are listed in Table 2.

Moreover, some advantages and disadvantages of this PCM are listed

Table 1
Materials used for experimental rooms' construction.

Material	Dimensions (cm)	Thermal conductivity (W/m.K)	Description
Roof:			
Isogam (roofing layer)	0.4 (thickness)	0.35	Isogam is local roofing material used for insulation and waterproofing. It has an external reflective layer to reflect as much as possible of solar radiation, minimising the heat transfer through the roof.
Concrete (main layer)	50 (thickness)	1.49	This layer is a popular main roof layer in the residential buildings in Iraq. It was fabricated according to the Iraqi construction pattern and governmental blogs. More details about the procedure and mixing ratio can be found in [43].
Gypsum mortar (cladding layer)	0.2 (thickness)	0.23	This is the popular interior cladding material for all building types in Iraq.
Walls:			
Concrete bricks (main layer)	23 (length) × 12 (width) × 7 (thickness)	1.4	This brick type is widely used in the northern regions of Iraq and is limitedly used in the hot southern regions due to its poor thermal performance. Details about the step-by-step procedure and mixing ratio followed to fabricate the bricks can be found in [45].
Cement mortar (cladding layer)	1 (thickness)	0.99	This layer is popularly applied on the exterior and interior wall surfaces in Iraqi buildings. In this work, the cement mortar layer was applied on the exterior walls to ensure no air leakage could enter the room through bricks joints.
Window			
Single glazing	0.6	/	A locally available clear single glazing window was fixed on the east wall of each room.

in Table 3, making it a good option in the current work. It is worth mentioning that this paraffin type is popular in Iraq and extensively used locally in different thermal applications such as solar desalination [48], electrical distribution transformers [49], solar air heating [50] and solar photovoltaic modules [51]. Moreover, this PCM has considerable potential to overcome the cooling load issues in Iraqi buildings during the summer period. It is particularly massively available in the Iraqi petroleum refineries as a waste product [52].

Macroencapsulation technique using widely available local metallic sheets was adopted to prepare the PCM panel for the roof and PCM capsules for wall bricks of the PCM room. These encapsulation materials are suitable for the application considering the thermal performance provided and compatibility with the PCM type [55]. The PCM panel used in the roof combination of the PCM room was made of galvanised steel sheet (0.5 mm thickness) with dimensions of 100 × 100 × 1.5 cm. According to our previous investigation, this panel thickness is the best-thermally performed under the exact location [44]. Although the panel could carry more than 10 kg of PCM, only 7 kg was poured inside the panel to ensure that no leakage occurs during the melting phase that may result from PCM volume change or possible panel inclination during installation.

For the walls of the PCM room, PCM capsules made of aluminium containers (1 mm thickness) of a square cross-sectional area of 4 × 4 × 2 cm dimensions were immersed inside each concrete brick. Five PCM capsules were inserted in the centre of each PCM concrete brick. Each PCM brick holds a total PCM quantity of about 145 g. These capsules are the best thermally-performed amongst many capsules of different shapes that were investigated in our previous studies [45,46]. Fig. 3 shows the preparation of PCM capsules and PCM bricks. More details about the step-by-step procedure followed to prepare the PCM bricks can be found in [45].

2.3. Energetic and thermal comfort investigation

Several indicators have been applied and discussed to show the thermal behaviour of the PCM room in comparison with the reference room. These indicators are classified into energetic and thermal comfort indicators.

The main energetic indicators presented are the maximum temperature reduction, average temperature fluctuation reduction, decrement factor and time lag. At the same time, the operative temperature difference, discomfort hours reduction and heat gain reduction are the main thermal comfort indicators considered in the study.

2.4. Measurement devices

T-type thermocouples were used to measure inside and outside surface temperatures of tested rooms in addition to the indoor and outdoor ambient temperatures. Thermocouples were fixed on the interior surface of each element of rooms, and others were fixed on the exterior surfaces of the reference room. Besides, one thermocouple was fixed inside each room at the middle with a suitable height to measure the air temperature inside rooms. All thermocouples were connected to a multi-channel Arduino (Mega 2560), which is programmed to measure and record temperatures with 10 min time step during the whole experimental period. The collected data is continuously stored in 4 GB flash memory and then exported to a PC at the end of the experiment. The solar radiation during daytime is measured every half an hour using a mobile high precision solar power meter. The schematic diagram and measurements details are shown in Fig. 4 and Table 4.

3. Results and discussion

3.1. Weather conditions and envelope surface temperatures

The experimental work was conducted for 24 h on 16th September 2021 under actual weather conditions of Al Amarah city (Latitude: 31.84° and Longitude: 47.14°), located in Southern Iraq. This month is among the hottest months in the country, characterised by high ambient temperature, high solar radiation, and long sunshine hours, as indicated in Fig. 5a. Moreover, it has been noticed that this temperature trend keeps high year by year [56], as shown in the historical data presented in Fig. 5b.

The measured outdoor ambient temperature and solar radiation on the experiment day are shown in Fig. 6. As indicated in the figure, the outdoor ambient temperature exceeded the mark of 47 °C in midday, with high solar radiation values exceeding 1200 W/m^2. Moreover, the ambient temperature exceeded 30 °C in the late night and early morning hours, indicating how needed HVAC systems are during the whole day in such locations to maintain suitable thermal comfort for residents.

Figs. 7-12 show the recorded inside and outside surface temperatures for the roof, east wall, north wall, west wall, south wall and the indoor ambient temperature of PCM and reference rooms, respectively, for the 24 h with a 10 min time step. The outdoor temperature recorded a minimum of 30.5 °C in the early morning and a maximum of 47.5 °C in the midday at 13:40. The maximum outdoor surface temperature reached 56.5 °C, 56 °C, 52.75 °C, 59.25 °C and 53.75 °C for the east wall,

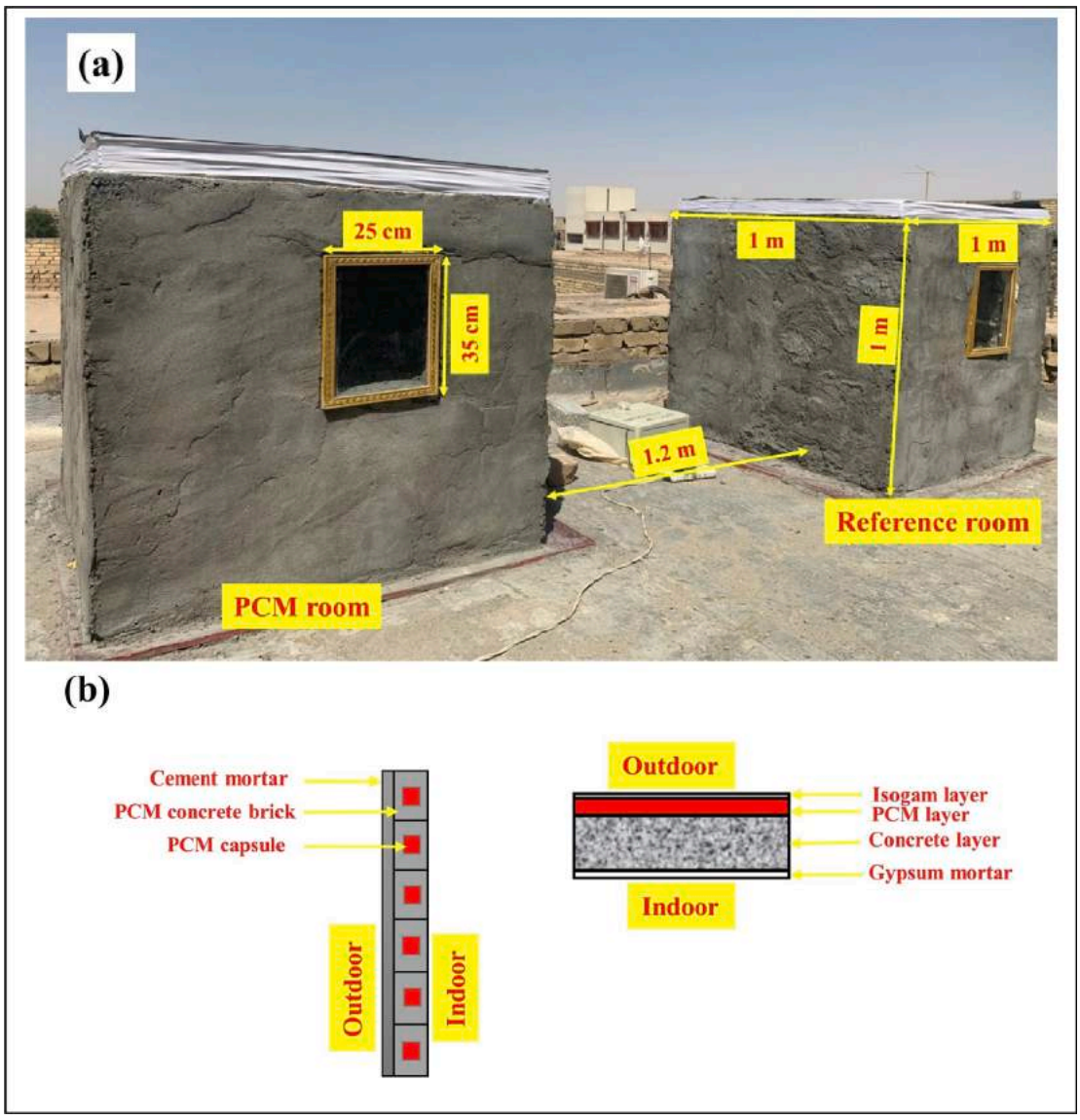

Fig. 1. Experimental set-up (a) 3D view of rooms, (b) cross-sections of PCM roof and wall.

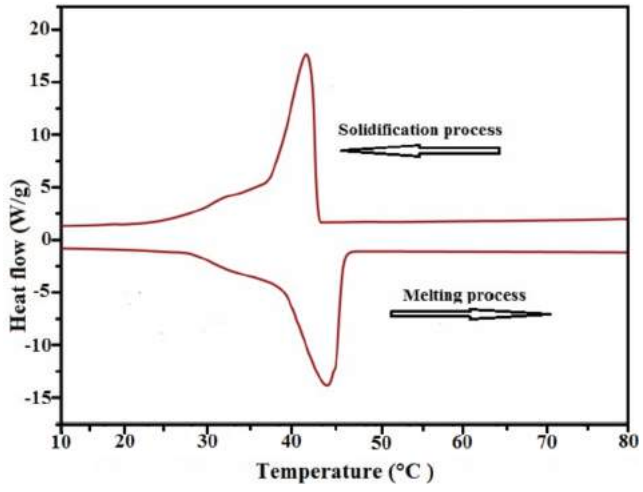

Fig. 2. DSC test of used paraffin wax (PCM).

Table 2
Characteristics of PCM used in the experiment.

Property/ feature	Unite	Value
Appearance	————	Whitish
Composition	%	40 oil + 60 wax
Melting temperature range	°C	40–44
Latent heat of fusion	kJ/kg	190
Thermal conductivity (solid & liquid)	W/m.K	0.21
Density (solid/liquid)	kg/m^3	930/830
Specific heat (solid & liquid)	kJ/kg.K	2.1

west wall, north wall, south wall and roof, respectively.

The east, west, north and south walls of the reference room reach maximum indoor surface temperature marks of 53.5 °C, 52.5 °C, 52.25 °C and 57.75 °C, respectively. In comparison, they recorded a maximum of 50.75 °C, 51.25 °C, 51.5 °C and 55.5 °C, respectively, in the PCM room. Moreover, the maximum indoor roof surface temperature and indoor ambient temperatures were 51.5 °C and 50.5 °C in the reference room compared with 48.25 °C and 49.25 °C in the PCM room.

It is evident from the figures that each element has its temperature variation trend depending on the time during the day and sun position.

Table 3
Advantages and disadvantages of used PCM [51–54].

Advantages	Disadvantages
- Locally available at a low price (it can also be provided free for research purposes by the government). - High thermal storage capacity. - Chemically stable after many thermal cycles. - Low flammability. - Compatible with many encapsulation materials. - Environmentally friendly (organic).	- Low thermal conductivity (common disadvantage of paraffins). - Paraffin solidification at the container edges may occur. - Crystallisation may occur after many melting/solidification cycles.

However, two intrinsic summaries are noticed in these figures, namely:

- All elements of the PCM room, more or less, have stable temperature behaviour than the reference room, which showed more temperature fluctuations. This fact is attributed to the PCM potential that traps the heat, making the envelope element more thermally stable against changeable weather conditions than local construction materials without PCM.
- The elements of the PCM room showed adverse thermal behaviour after sunset (after 18:00 till the beginning of the next day), in which the inside surface temperature of all elements was increased. This is mainly due to the PCM inclusion in the PCM room with a non-conditioned case wherein the stored heat starts to transfer towards the outdoor low ambient temperature during the peak period.

It is also worth mentioning that roofs' thermal behaviour is different from the walls during the night period. As indicated in Fig. 7, the roofs' inside surface temperatures stay with a remarkable gap till the end of the next day. This is because the roof has more layers than walls, so the heat needs more time to be released from the PCM roof than walls.

At night, mainly soon after 18:00, the indoor surface temperature of PCM room elements was higher than that of the reference room. This means that PCM starts releasing its heat as the ambient temperature falls, and it needs an average of 6–8 h to discharge all stored heat [58]. Besides, the non-conditioned/ventilated rooms slowed the heat release from the indoor environment to the outdoor ambient, which is undoubtedly faster in the ventilated cases. Therefore, ventilation is recommended for passive PCM building applications under hot locations [59].

3.2. Rooms' energetic assessment

Energy-saving earned from PCM incorporation into building envelopes is a commonly studied topic in the literature on a seasonal or annual basis [60,61]. However, a detailed energetic analysis can be made for a shorter period considering several indicators showing the main advantages of PCM in terms of the interior and exterior temperatures of the reference and PCM rooms. In this study, several energetic indicators were adopted to show the thermal behaviour of the PCM room against the reference room, such as the maximum temperature reduction, average temperature fluctuation reduction, decrement factor and time lag.

3.2.1. Maximum temperature reduction

Maximum temperature reduction (MTR) describes how high is the temperature reduction of room's elements considering the indoor and outdoor surface temperature of each element in the PCM room compared with the reference one. Mathematically, the MTR of the roof, for example, could be calculated according to Eq. (1), as follows [37]:

$$MTR = T_{R,max.} - T_{r,max.} \quad (1)$$

where $T_{R,\max.}$ and $T_{r,\max.}$ are respectively the maximum surface temperature of the outdoor and indoor roof in °C. Moreover, the MTR difference between elements of reference and PCM rooms can also be calculated to show the contribution of PCM to the element energy

Fig. 3. Preparation of PCM bricks: (a) aluminium capsules; (b) pouring of liquid PCM; (c) solidified PCM capsules; (d) capping of PCM capsules; (e) PCM capsules inside concrete during preparation; (f) dried PCM bricks.

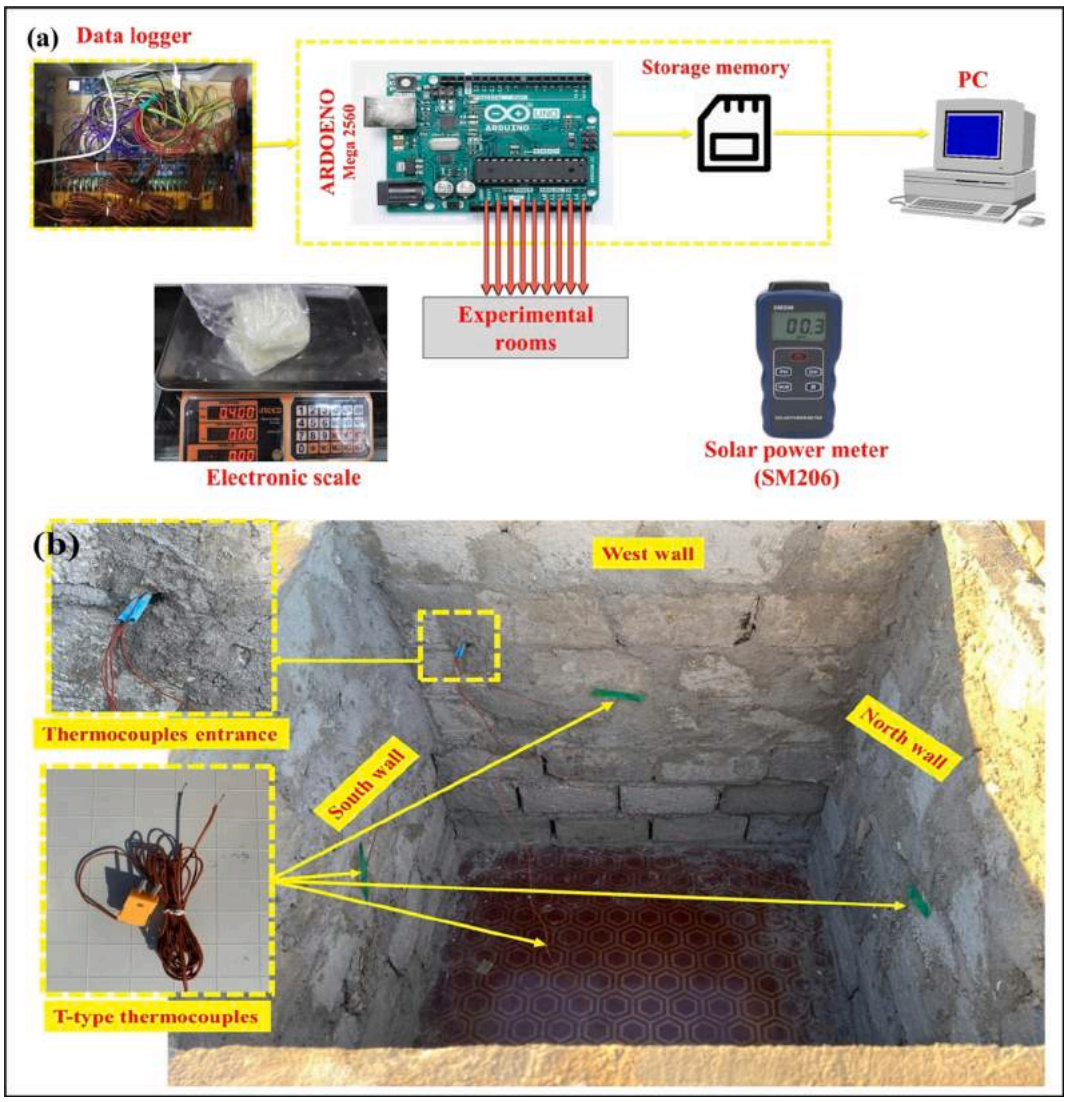

Fig. 4. (a) Schematic view of measurement procedure and devices, (b) view for the reference room showing the position of thermocouples on internal wall surfaces.

Table 4
Specifications of measurement devices as indicated by the manufacturer.

Measurement device	Model	Range	Resolution	Accuracy
Thermocouples T-type (0.2 mm)	TEMPSENS	−270 °C – 370 °C	———————	±0.5 °C
Solar power meter	SM206	0.1 ~ 399.9 W/m^2	0.1 W/m^2	±10 W/m^2

enhancement.

Fig. 13 represents the MTR of each element of reference and PCM rooms together with the MTR difference for each element. As observed in the figure, the east wall, followed by the south wall, show the highest MTR and MTR difference compared with other walls. Moreover, the roof showed the highest MTR and MTR difference compared with walls.

The MTR of east, west, north and south walls in the reference room was 3 °C, 3.5 °C, 0,5 °C and 2 °C compared with 5.75 °C, 4.75 °C, 2 °C and 4.25 °C in the PCM room, respectively. Moreover, the MTR of the roof in the reference room was 2.25 °C compared with 5.5 °C in the PCM roof.

The MTR difference between the reference and PCM rooms are 2.75 °C, 1.25 °C, 1.5 °C, 2.25 °C and 3.25 °C, respectively for the east wall, west wall, north wall, south wall and the roof. These MTR difference values influence the thermal comfort inside the room and energy consumed during the peak period. Besides, they indicated positive energetic behaviour although the rooms were built with limited sizes and with no ventilation.

It is known that the MTR of the roof and walls all influence the indoor temperature inside the rooms. Accordingly, MTR can be calculated for indoor air of both rooms, considering the difference with the outdoor ambient temperature. MTR difference of indoor air inside the PCM room compared with the reference one (also researchers referred to as indoor temperature reduction (ITR) or indoor temperature drop) ranged between 0.25 °C and 5.75 °C during day hours. These values align with those of studies verified under hot weather conditions. For instance, Sovetova et al. [62] conducted a numerical study under hot weather of Sharjah and Al-Ain cities in the United Arab Emirates and found that the optimal PCM can decrease the MTR by up to 1.09 °C when incorporated with the building envelope. Moreover, recent studies found that ITR reached about 0.2 °C to 4.3 °C under Indian hot weather conditions [63] and about 3.4 °C under Danish summer conditions [64].

3.2.2. *Average temperature fluctuation reduction*

Average temperature fluctuation reduction (ATFR) is the average

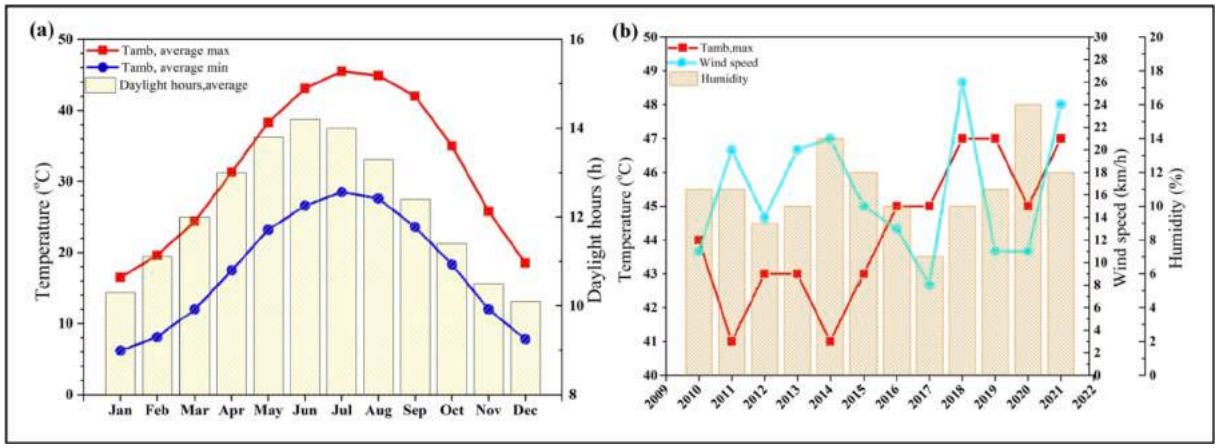

Fig. 5. Historical weather conditions of the site under study [57] (a) Average maximum and minimum ambient temperature and daylight hours by month in 2021; (b) maximum ambient temperature, wind speed and humidity for September during the last 12 years.

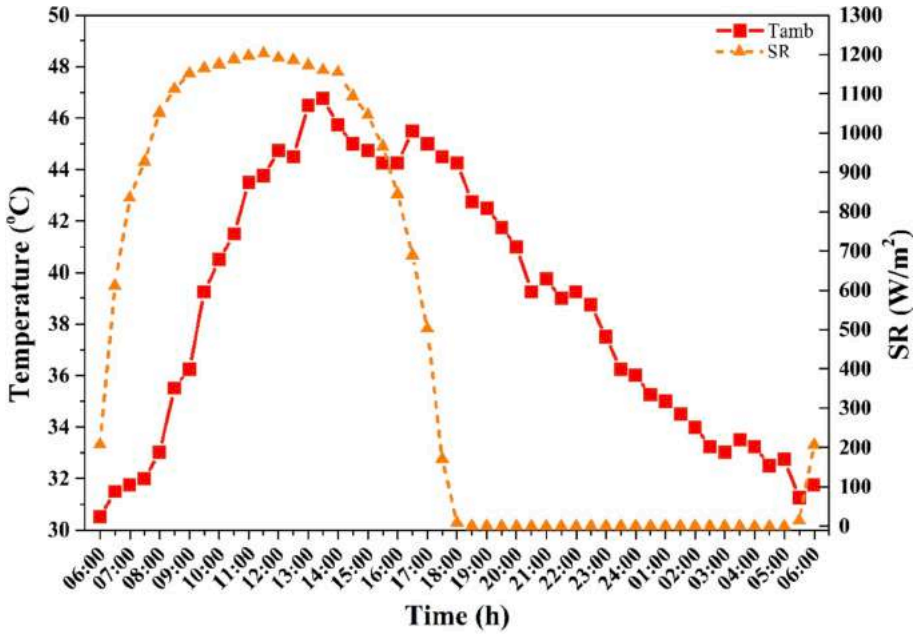

Fig. 6. Outdoor ambient temperature (Tamb) and solar radiation (SR) during the experimental day measured in-site.

reduction in the envelope element layers temperature considering the interior and exterior temperatures during the whole day cycle. In other words, ATFR is the summation of the average decrease in the envelope temperature during the daytime and the average increase in the envelope element temperature during the nighttime (as a result of non-ventilation). Therefore, the higher the ATFR value, the better the thermal behaviour of PCM (the negative value of ATFR means that the PCM incorporation has adverse thermal behaviour, while zero value means no advantages of PCM incorporation). In this work, the period from 6:00 to 18:00 represents the daytime (denoted by *X*). The period from 18:00 to the end of the cycle denoted by *Y* represent the nighttime. ATFR was calculated according to Eq. (2)-Eq. (4) [65], as follows.

$$ATFR = X + Y \tag{2}$$

$$X = T_{av.,ref.} - T_{av.,PCM} \tag{3}$$

$$Y = T_{av.,PCM} - T_{av.,ref.} \tag{4}$$

where $T_{av.,ref.}$ and $T_{av.,PCM}$ are respectively the average temperature of the element of the reference and PCM rooms in °C.

ATFR calculation results are presented in Fig. 14. ATFR of the PCM room roof was much higher than all walls. The maximum ATFR of east wall, west wall, north wall, south wall and the roof were ~ 2.4 °C, ~2.3 °C, 3.3 °C, 2.1 °C and 6.5 °C, respectively. Moreover, the ATFR of the indoor air of the PCM room compared with the reference one reached 3.45 °C, influenced by the values obtained for the room's elements. This value reflects the remarkable advantage of incorporated PCM as it was exceeded the mark of 3 °C [66]. Alam et al. [65] found that ATFR ranged between 3 °C and 4 °C in tested PCM-enhanced envelope in different Australian cities (Canberra, Melbourne and Hobart) from September to April. Kenzhekhanov et al. [37] verified ATFR values between 1.59 °C and 2.65 °C during the summer season of different cities worldwide, namely Bratsk, Arkhangelsk and Surgut in Russia, Fort McMurray and Val-d'Or in Canada, Oulu in Finland, Umea in Sweden and Anchorage in the United States.

The figure shows that the PCM incorporation was beneficial as all ATFR values were more than 0 °C. This means that all X-values were higher than Y-values in every element, indicating the better performance of PCM during the daytime. Fig. 14 also indicates a negative Y value for the east wall of the PCM room, which was the best-thermally

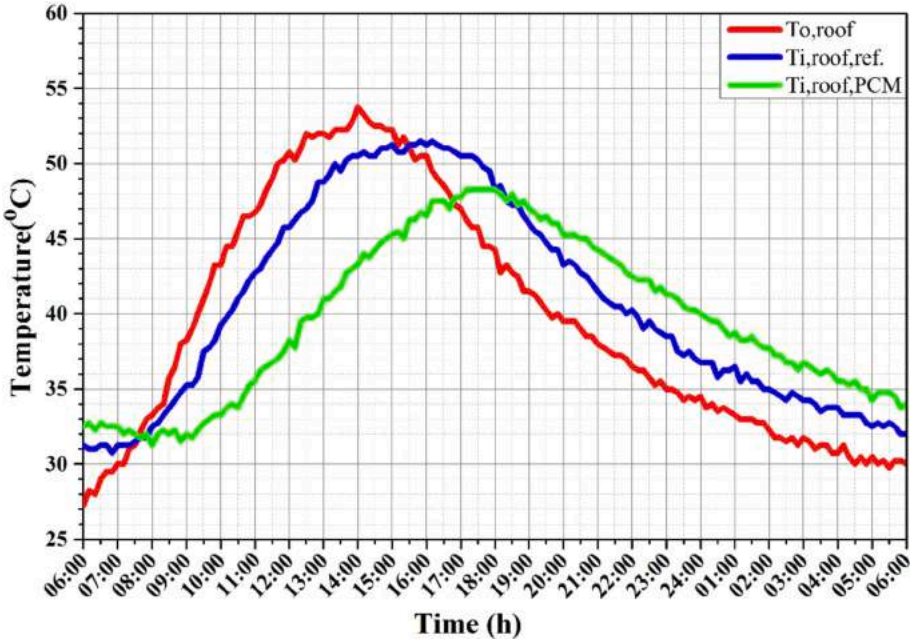

Fig. 7. Roof surface temperatures of reference and PCM rooms.

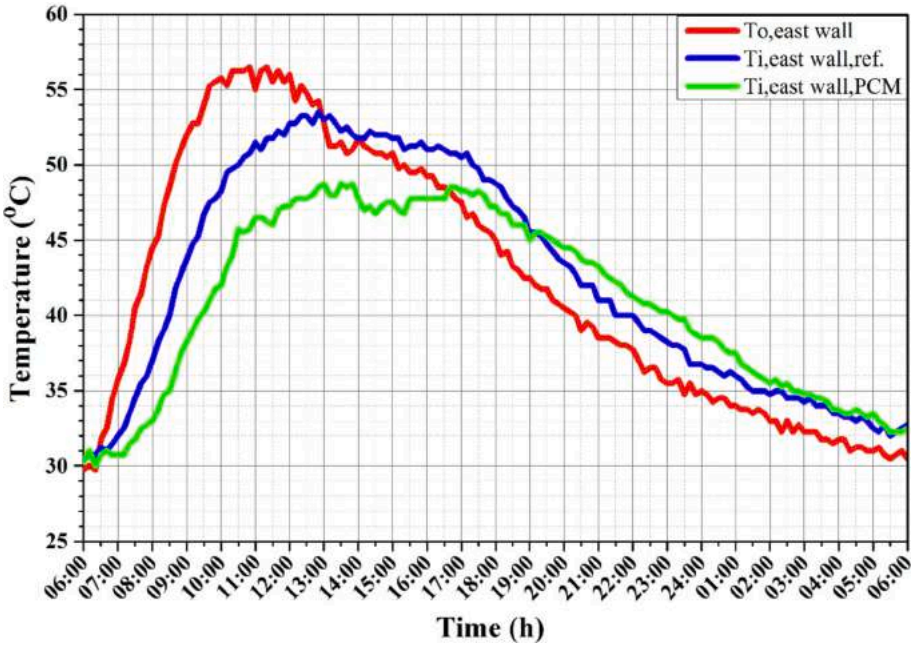

Fig. 8. East wall surface temperatures of reference and PCM rooms.

performed amongst walls in terms of MTR. This proves that the east wall had stored more heat than other walls during daytime which remained with high temperature for a longer time. However, its X-value was much higher than other walls as ATFR deals with the temperature difference between the reference and PCM rooms during the day and night.

3.2.3. Decrement factor

Decrement factor (DF) is the reduction in the cyclic temperature through the envelope elements [67]. This means that the envelope element with a lower DF has a higher thermal resistance against the outdoor temperature fluctuations. This property is essential for the thermal comfort assessment as it is associated with the mean radiant and operative temperatures. The DF was calculated as the difference between the element's maximum and minimum interior surface temperatures to the difference between the maximum and minimum exterior surface temperatures. For instance, the DF of roofs was calculated according to Eq. (5) [68]. All other elements followed the same formula.

$$DF = \frac{T_{r,max} - T_{r,min}}{T_{R,max} - T_{R,min}} \tag{5}$$

where $T_{r,\max}$, $T_{r,\min}$, $T_{R,\max}$ and $T_{R,\min}$ are respectively the maximum and minimum temperatures of the interior and exterior roof surfaces in °C.

The calculation results of DF for the reference and PCM rooms are shown in Fig. 15.

Generally speaking, PCM room elements showed better DF, as expected, thanks to the PCM thermal potential, which literarily worked as

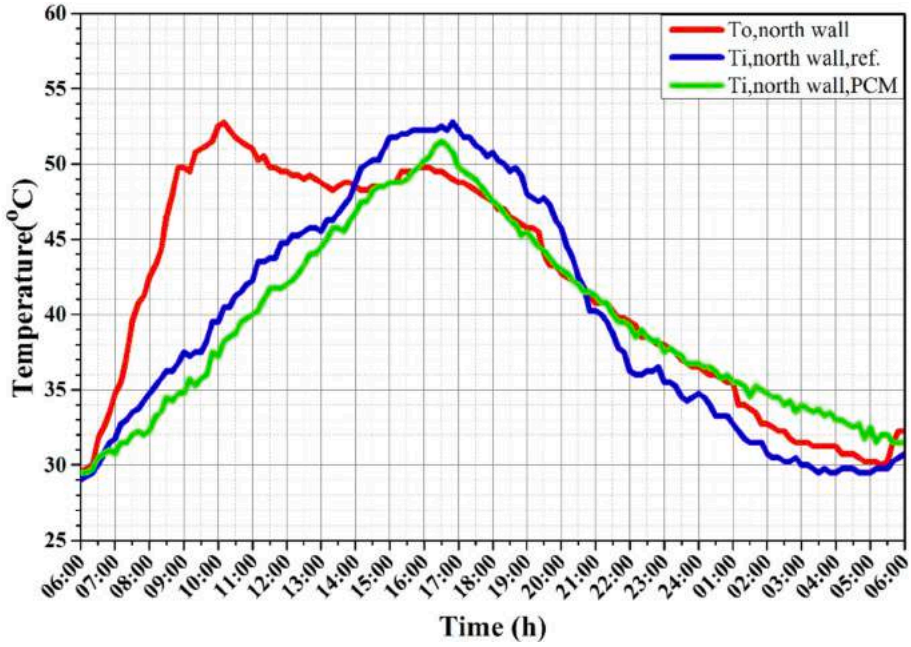

Fig. 9. North wall surface temperatures of reference and PCM rooms.

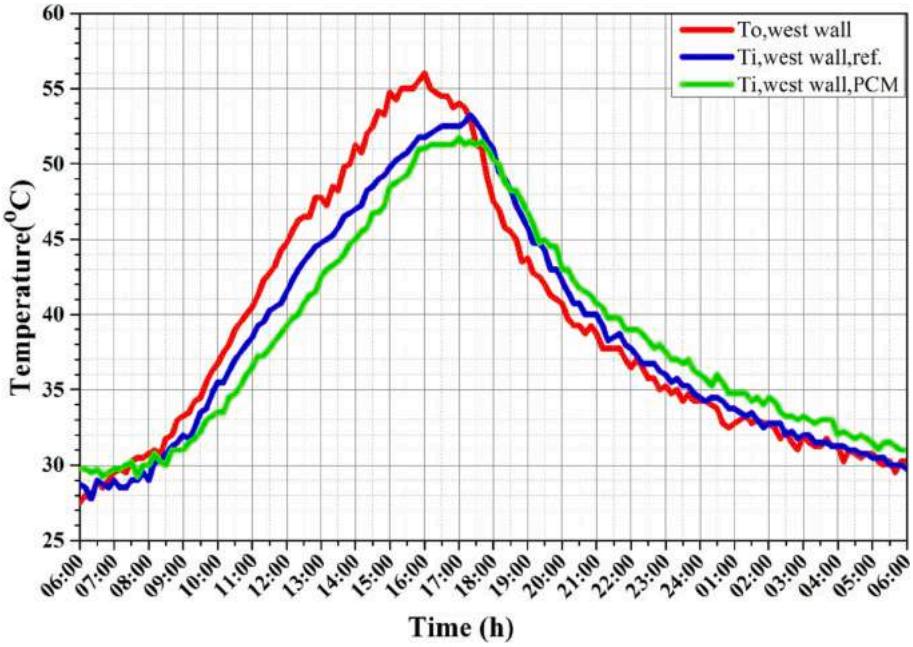

Fig. 10. West wall surface temperatures of reference and PCM rooms.

dynamic insulation. The DF reduction of the east wall, west wall, north wall, south wall and the roof of the PCM room was better than the reference room by about 12.8%, 11.7%, 12.5%, 13.3% and 25.6%, respectively. DF of the PCM room roof was almost double of each wall, indicating the better performance of PCM in the roof compared with walls. This is mainly due to the better thermal performance of the roof's layers and the position of the PCM in the roof close to the outdoor environment, which charge and discharge heat far from the indoor environment, compared with the middle position in walls. Saafi and Daouas [69] confirmed this fact, reporting that the DF of a PCM applied on a north wall was reduced from 39.41% to 27.3% by changing the PCM position from internal to an external location (close to the outdoor environment). On the contrary, Jia et al. [69] claimed that PCM filled the inner cavities of concrete blocks had reduced DF from 12.3% to 17.0% to 1.7%–2.2%. In another approach, Kontoleon et al. [70] studied the effect of PCM thickness on the DF and found that the PCM-enhanced cement mortar can reduce the DF of a standard concrete wall by 17.4%, 22.1% and 29.1% when 1, 1.5, and 2 cm of PCM layers applied, respectively.

3.2.4. *Time lag*

The difference between the time at the maximum interior and exterior element surface temperatures is identified as the time lag (TL). TL indicates the shifting of peak temperature during the midday to the off-peak period at a late time, which is the main benefit of PCMs in building applications. Accordingly, the TL of the roof element was calculated

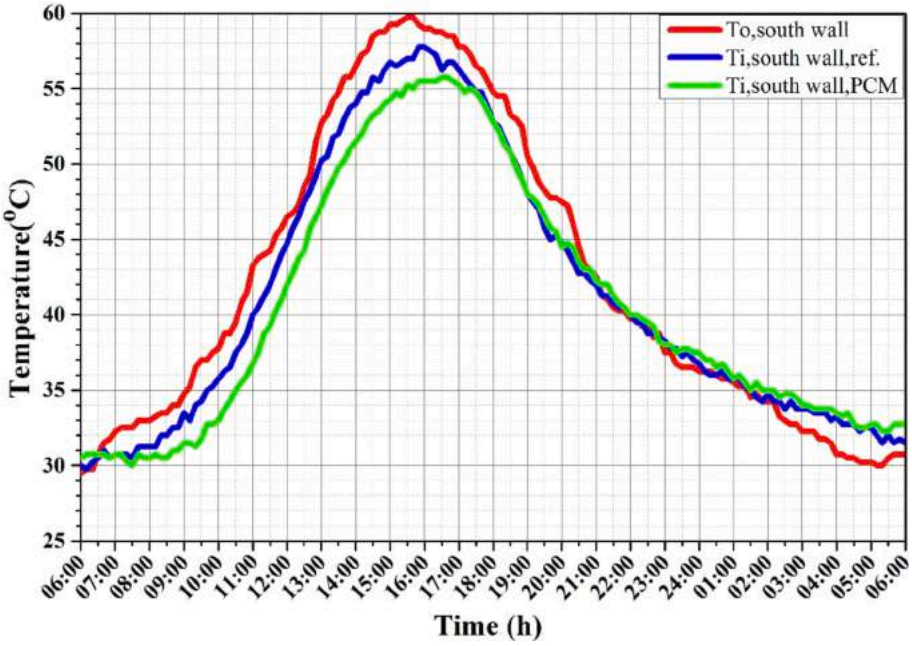

Fig. 11. South wall surface temperatures of reference and PCM rooms.

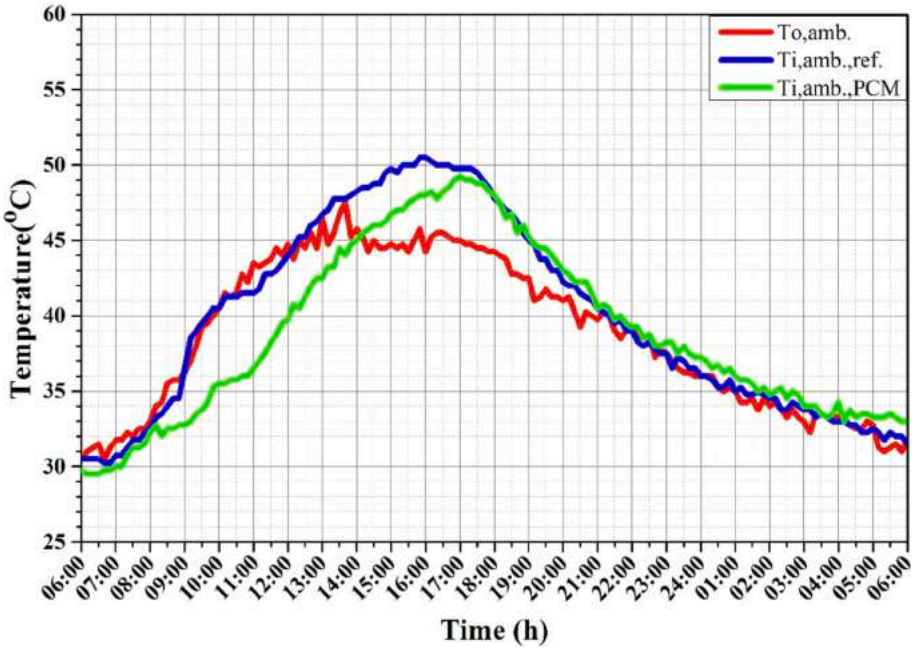

Fig. 12. Outdoor ambient temperature against indoor temperatures of reference and PCM rooms.

according to Eq. (6) [71]. TL of all other elements was calculated following the same formula.

$$TL = \tau_{T_{r,max}} - \tau_{T_{R,max}} \quad (6)$$

where $\tau_{r,\max}$ and $\tau_{R,\max}$ are respectively the time at the maximum interior and exterior roof surface temperatures in min.

Fig. 16 shows the TL and TL difference in the reference and PCM rooms' elements.

As shown in Fig. 16, the TL is different from one element to another. For instance, the north wall had the maximum TL among other walls by 320 and 340 min in the reference and PCM rooms. This TL is quite large and is not logical compared with other rooms' elements. By considering the temperature trend of the outdoor surface temperature of the north walls presented in Fig. 9, we recognise that the maximum outdoor surface temperature reached around 10:00 in the morning, as expected as the solar radiation was high near the north walls in the early morning hours. In contrast, the maximum indoor surface temperature of north walls was reached after 16:00, in the afternoon, due to the accumulated heat during the whole day and the influence of the other elements' temperature on it due to the non-ventilated conditions.

On the other hand, a more logical explanation can be observed when considering the TL difference between the reference and PCM rooms. In this regard, the east wall followed by the south walls had the maximum TL difference (40 min and 30 min, respectively) compared with the west and north walls that had only 20 min. This is expected as long as the east

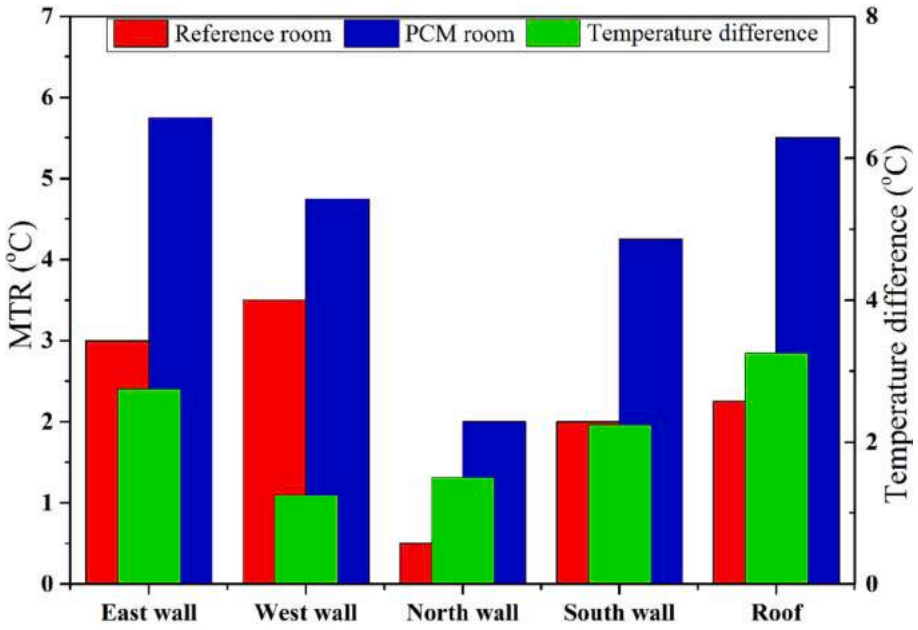

Fig. 13. MTR of reference and PCM rooms' elements.

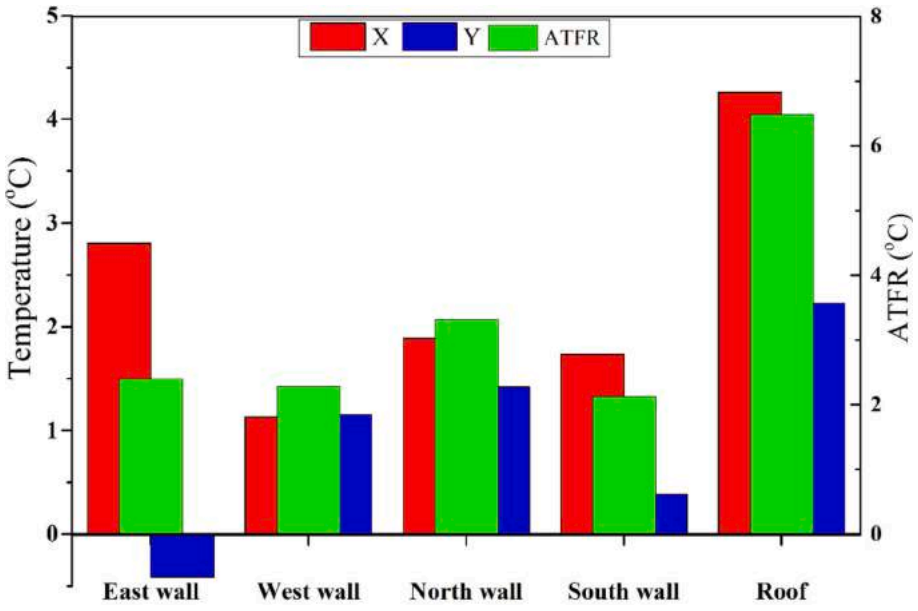

Fig. 14. ATFR of reference and PCM rooms.

and south walls experienced direct high solar radiation for a longer time than the other walls, in which the PCM was activated sufficiently. The MTR indicator also supports this, which shows the best thermal behaviour of east and west walls. Moreover, the roof of the PCM room showed the highest TL difference/increment with 70 min compared with the roof of the reference room. Wu et al. [72] exhibited that applying PCM on walls resulted in TL in the range 3.33 h- 4.17 h and was affected by the thickness and position of PCM. In this regard, Zhang et al. [73] stated that TL of PCM incorporated hollow concrete brick wall was reduced by 0.5 h- 3 h under China weather conditions depending on the PCM position within the bricks. In the same approach, Jia et al. [69] claimed that PCM filling the interior gaps of concrete bricks can reduce the TL from 1.50 h to 2.00 h to 6.17 h- 6.50 h under Shanghai city weather conditions. Another study showed that TL was decreased by 0.14 h, 0.66 h, and 1.30 h when 5, 10 and 15 mm PCM thickness was incorporated compared with a base case with no PCM [74]. Imghoure et al. [75] found that the TL for building wall incorporated Bio-PCM ranged from 2 h to 3 h compared with the base case regardless of PCM thickness and position under the summer climate of the Marrakech region.

3.3. *Thermal comfort analysis*

Thermal comfort gained from PCM incorporation has limited attention by researchers in the literature as most PCM investigations focus on energy-saving requirements [76]. Therefore, this work considers three important thermal comfort indicators: operative temperature difference, discomfort hours reduction, and maximum heat gain reduction.

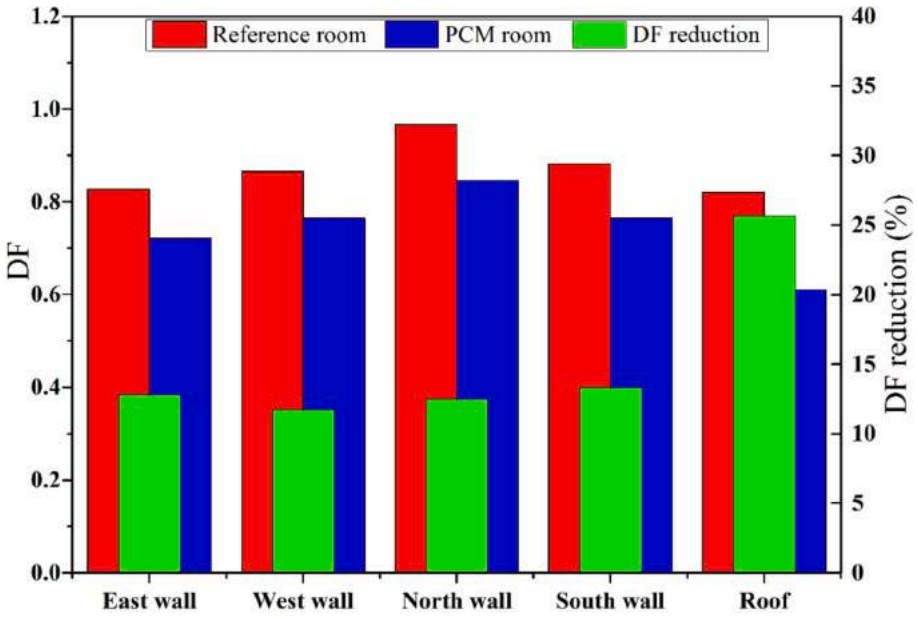

Fig. 15. DF of reference and PCM rooms.

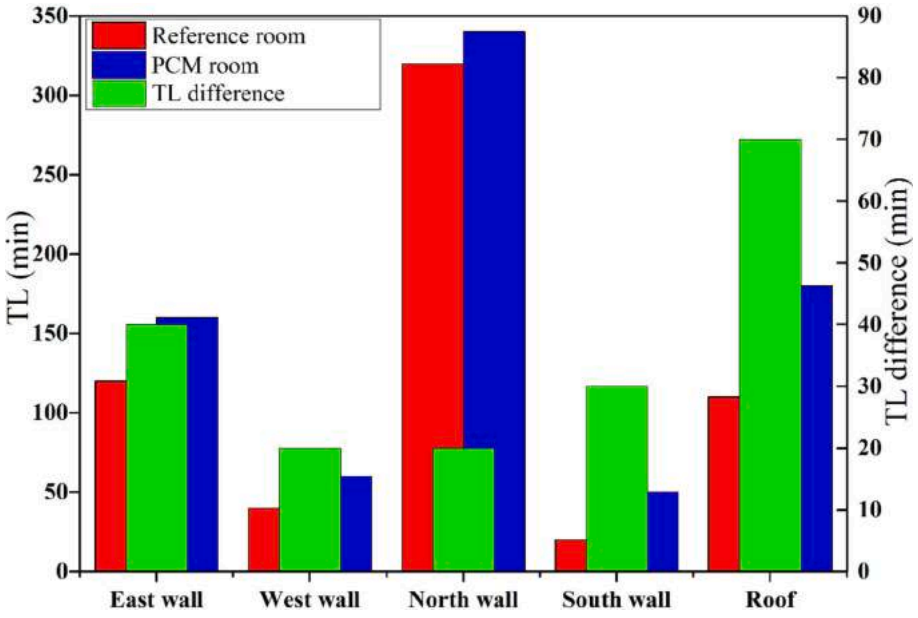

Fig. 16. TL of reference and PCM rooms.

3.3.1. Operative temperature difference

The operative temperature (OT) is the temperature that occupants feel inside the built environment. Mathematically, OT can be defined as the average indoor air and mean radiant temperatures, calculated by Eq. (7) [77], as follows:

$$OT = \frac{T_a + \overline{T}_{mr}}{2} \tag{7}$$

where T_a is the indoor ambient temperature (i.e., Ti in the current research) and, $\overline{T}_{mr}$ is the mean radiant temperature (both in °C). The latter can be calculated by considering the indoor surface temperatures and areas of roof and walls, according to Eq. (8) [78].

$$\overline{T}_{mr} = \frac{T_1A_1 + T_2A_2 + \cdots + T_nA_n}{A_1 + A_2 + \cdots + A_n} \tag{8}$$

where T_1, T_2, …, T_n are the element interior surface temperatures in °C, and A_1, A_2, …, A_n are respectively the interior area of each element in m^2.

Fig. 17 shows the OT variation of the reference and PCM rooms against the outdoor ambient temperature.

The figure designates that outdoor ambient temperature was higher than the OT in both rooms till around noon. It then gets lower as the interior surface temperature of rooms' elements increases with a noticeable time delay between the PCM and reference room. Moreover, the heat accumulated inside rooms throughout the experiment (due to non-ventilation) continuously increases the indoor air temperature. It was also evident that the OT of the PCM room was lower than that of the reference room during the daytime, and the trend reversed in the evening (after 18:00) till the next day. This is attributed to PCM integration into elements that release their heat uncontrollably as the ambient

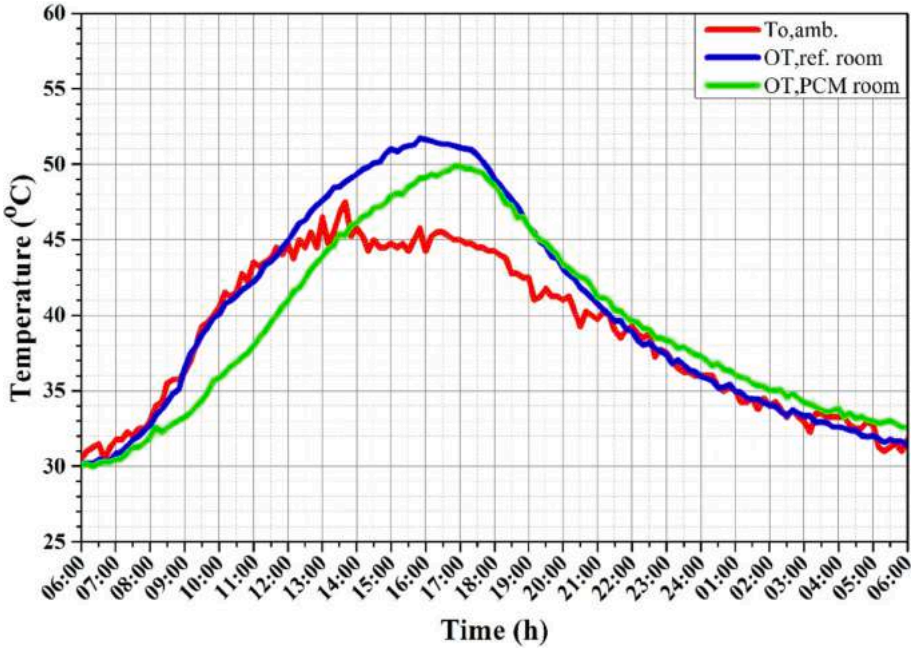

Fig. 17. OT variation of reference and PCM rooms.

temperature falls below 44 °C during the day. The maximum OT difference reached 4.6 °C at 10:10 due to the PCM activation involved in the PCM rooms' elements that were the most in the period from 9:20 to 11:30. This period is critical in actual buildings in Iraq as it represents the peak period of electric power consumption for powering air-conditioning systems. Besides, the rooms required suitable ventilation in the period after sunshine to overcome the indoor temperature increment that occurs due to the PCM heat discharging phase. The OT difference/reduction results obtained in the current work are remarkable compared with those found in the literature. For instance, Costanzo et al. [42] conducted a study under three different climates, namely Rome (Italy), Wien (Austria) and London (United Kingdom), to show the effectiveness of commercial PCM-enhanced office building walls considering the OT reduction. Numerical results exhibited OT reduction by 0.5 °C at the day hours in a conditioned environment. Al Touma and Ouahrani [79] examined the thermal behaviour of PCM incorporated floor and wall tiles applied to typical Majlis living space in Qatar. Results showed that the PCM enhanced the space OT that was in the range from 25.7 °C to 29.4 °C and became in the range of 26.1 °C to 29 °C after PCM incorporation, indicating OT enhancement by 21.6% on average. Ramakrishnan et al. [80] conducted an experimental and numerical study for form-stable PCM-enhanced plastering mortar applied as a cladding layer for a multi-story office building in Milbourn, Australia. Considering the OT, results indicated that the applied method reduced the indoor OT by up to 2.5 °C. The above literature studies indicate that the PCM macroencapsulated panel and capsules adopted in the current study was more effective than other incorporation methods. However, this effectivity could be more improved when dealing with the negative behaviour at night, as stated by Adilkhanova et al. [82] that OT could be enhanced by more than 5 °C with a suitable night cooling control under all conditions cities of Kazakhstan.

3.3.2. Discomfort hours reduction

According to the OT analysis described in the last subsection, the daytime thermal behaviour is essential in this study as it shows the benefits of PCM incorporation. According to ASHRAE standard 55–2004, discomfort hours are defined as when occupants are not satisfied thermally inside buildings considering the temperature and humidity levels [81]. Therefore, the discomfort hours reduction (DHR) identifies the discomfort period inside buildings (in hours). This indicator measures the improvement of thermal comfort due to incorporating PCMs. The temperature variation (shown in Fig. 6) designated that the outdoor ambient temperature was always above 30 °C during the day, meaning that the thermal comfort level cannot be obtained without applying air-conditioning means. Therefore, the discomfort hours cannot be identified in this case. However, the OT reduction in the PCM room compared with the reference room could be considered, which has an equivalent indication of the DHR [37]. The DHR was calculated according to Eq. (9), as follows [37]:

$$DHR = \frac{OT_{ref.room} - OT_{PCMroom}}{OT_{ref.Room}} \times 100\% \quad (9)$$

The hourly DHR resulting from the PCM incorporation into the PCM room during the daytime is listed in Table 5.

According to Table 5, the maximum DHR was reached in the first half of the day between 10:00 and 11:00 in the range of 10.1% to 11.2%. This period experienced high solar radiation and outdoor temperature levels, as the PCM inside the roof and walls in the heat charging phase. In contrast, the DHR is getting low in the late afternoon, during which the outdoor ambient temperature gets lower than the melting temperature of PCM. Thus, the heat discharging phase of PCM starts with no control on heat dissipation towards the indoor environment, and the OT of the

Table 5
Hourly OT and DHR of reference and PCM rooms.

Time (h)	$OT_{ref.\ room}$ (°C)	$OT_{PCM\ room}$ (°C)	DHR (%)
06:00	30.20	30.13	0.25
07:00	30.85	30.45	1.30
08:00	32.70	31.93	2.37
09:00	36.45	33.23	8.85
10:00	40.08	35.85	10.54
11:00	42.25	37.98	10.12
12:00	44.95	40.95	8.90
13:00	47.6	43.85	7.88
14:00	49.33	46.13	6.45
15:00	51	47.9	6.08
16:00	51.65	49.10	4.94
17:00	51.08	49.9	2.31
18:00	49.03	48.60	0.87

PCM room increased near to that of the reference room. DHR results above are reasonable under hot weather conditions due to high outdoor ambient temperature compared with the indoor environment, and higher percentages can be expected under lower outdoor temperatures. For instance, Maleki et al. [82] found out that applying PCM-enhanced plaster wallboards resulted in DHR by up to 13.83% under the climate of Tabriz, Iran. Whereas, a study by Jamil et al. [83] reached DHR up to 34% from passive PCM incorporated ceiling at Australian (Melbourne) weather conditions and further improved by up to 65% when a suitable air ventilation system was engaged under same weather conditions [84].

3.3.3. Maximum heat gain reduction

The solar heat gain reduced through the building envelope indicates the cooling load reduction [85]. Subsequently, this also specifies the energy-saving obtained from PCM incorporation [86]. The heat gain (HG) of each element in the reference and PCM room was calculated according to Eq. (10) [87], as follows:

$$HG = h_i A(T_{in} - T_r) \tag{10}$$

Where h_i denotes the combined convective and radiative heat transfer coefficient for the interior element surface and interior room temperature in W/m^2.K. In this study, the values 8.29 W/m^2.°C and 6.13 W/m^2.°C are used for walls and roofs, respectively, considering the horizontal/vertical direction of heat flow and surface emittance of concrete [88]. T_{in} and T_r refer to the inside element surface temperature and the interior air temperature, respectively. T_r is variable in this study because it is influenced by the heat exchange between the indoor and outdoor temperatures through the envelope elements. Sometimes it becomes higher than T_i due to the influence of non-ventilated space, giving adverse results. Therefore, it should be fixed in the calculations refereeing to the design temperature controlled by air-conditioning systems [89] (T_i assumed to be equal to 24 °C).

Consequently, the maximum heat gain reduction (MHGR) can be calculated considering the maximum HG in each element in the PCM room and its corresponding element in the reference room according to Eq. (11) [90], as follows:

$$MHGR = \frac{HG_{ref.} - HG_{PCM}}{HG_{ref.}} \times 100\% \tag{11}$$

Fig. 18 shows the MHGR in each element considering the HG of PCM and reference rooms.

Generally speaking, the figure above showed that the east wall had better HG compared with the other walls, followed by the south walls. However, the latter exhibited more HG in reference and PCM rooms. This indicates that the heat across these walls was high as they were exposed to high solar radiation for a long time, which allowed more heat to transfer. On the other hand, the roof of the PCM room minimised the HG more than that of the reference room thanks to the PCM layer, which interrupted the heat flowing towards the indoor zone. Considering the MHGR, the east and south walls showed MHGR of 9.3% and 6.7%, respectively. These percentages are higher than those of the west and north walls, which showed only 4.4% and 2.7%, respectively, indicating that these walls received less solar radiation, particularly the north wall. In contrast, the roof showed the best MHGR of about 11.8%.

The calculations show that the roofs had reduced the HG more than walls. This is mainly due to the thicker roof combination than the walls, which provides more thermal resistance against the heat flow. In addition, the PCM quantity incorporated into the roof was higher than that incorporated walls (7 kg in the roof against ~ 4 kg in each wall). Thus, more heat would be stored in the PCM roof than PCM walls, especially since the roof was exposed to direct solar radiation longer than any wall. In view of that, the total MHGR in the PCM room was about 34.8% compared with the reference room. This percentage is realistic compared with those obtained under different locations worldwide. For instance, the MHGR ranged by 3.5%–47.2% according to a study conducted under weather conditions of the United States [91], and by up to 35% under Saudi Arabia's climate conditions [92]. Besides, an optimisation study for building with insulation and PCM reported 33.5% MHGR under hot Indian climate conditions [93].

In addition to the above, Table 6 lists the results obtained in the current study and main findings of experimental literature studies conducted under similar hot climates to shed light on the main differences resulting mainly from diverse PCM incorporation methods and different locations.

4. Conclusion

In this paper, the thermal behaviour of a PCM incorporated thin building envelope was studied experimentally under Al Amarah city severe hot climate, southern Iraq. Two rooms, one with PCM and the other for reference, were built and tested during a typical hot summer

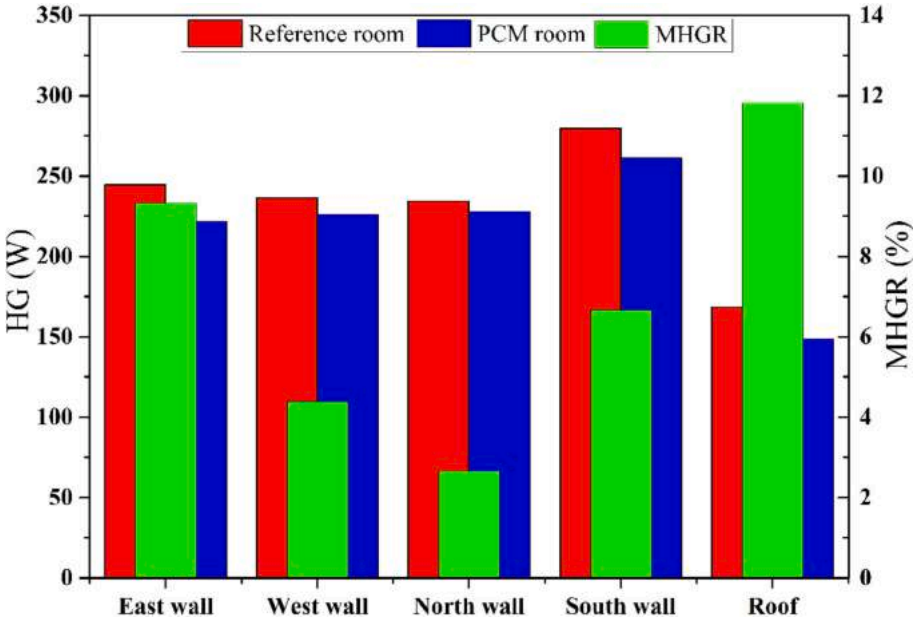

Fig. 18. HG and MHGR in the reference and PCM rooms.

Table 6
Summary of results obtained from other experimental studies published in the literature compared with the current study results.

PCM (melting temperature,°C)	Study location	PCM incorporation method	PCM position	Examined factors	Main findings	Ref.
SavE® OM37 (36–40)	India (Mathura)	PCM macroencapsulated aluminium pipes buried inside concrete roof and walls	Roof and walls	ITR, TL and HTR	ITR by 9.18%-19%, TL by 60–120 min and HTR by 0.67%-59.79%.	[36]
HS29 (26–29)	India (Chennai city)	PCM macroencapsulated foil packets inserted inside hollow bricks	Walls	ITR	ITR form 2 °C to 6 °C.	[94]
$CaCl_2{\cdot}6H_2O$/ expanded graphite (27.11)	China (Ningxia province)	Composite PCM macroencapsulated panel (2–14 mm thickness)	Roof and walls	ATFR, TL, DF and heat transfer reduction (HTR)	ATFR by 7 °C, TL by 1.4 h, DF by 0.378% and HTR by 13.4% were achieved under 8–10 mm thickness.	[95]
Paraffin wax (44)	Iraq (Kut city)	PCM macroencapsulated aluminium frame (1 and 2 cm thickness)	Inner edge of the roof and walls	ITR and cooling load reduction (CLR)	Maximum ITR by 2.18 °C and CLR by 20.9% were achieved at 1 cm PCM frame thickness.	[96]
Paraffin wax (40–44)	Iraq (Baghdad city)	PCM macroencapsulated panel (2.5 cm thickness)	Roof and east, west and south walls	Heat flux reduction (i.e., HTR)	HTR by 46.71%.	[97]
Paraffin wax (40–44)	Iraq (Baghdad city)	PCM macroencapsulated panel (2.5 cm thickness installed on the three walls and a panel of 2.5, 4 and 6 cm installed on the ceiling)	Roof and east, west and south walls	Heat flux reduction (i.e., HTR)	HTR by 38.45% was achieved with 6 cm thickness.	[98]
Paraffin wax (40–44)	Iraq (Al Amarah city)	PCM macroencapsulated panel (1.5 cm thickness) in the roof and macroencapsulated capsules inside concrete bricks	Roof and all walls	MTR, ATFR, DF, TL, OTD, DHR and MHGR	ITR by 0.25 °C-5.75 °C, ATFR up to 6.5 °C, DF by 11.7%-25.6%, TL increment up to 70 min, OT reduction by up to 4.6 °C, DHR up to 11.2% and total MHGR by 34.8%.	Current study

day in September 2021. The main design parameters, such as the best position and thickness of the PCM layer in the roof and the best encapsulation method for PCM capsules inside concrete bricks, were considered when constructing the rooms considering our preliminary experiments. A set of energetic and thermal comfort indicators were studied to show the thermal advancements of the PCM. Some conclusions can be drawn from the study can, as follows:

- The PCM considerably enhanced the thermal performance of the PCM room compared with the reference room during hot hours.
- The roof of the PCM room had better thermal performance than the walls. The MTR difference, ATFR, DF, and TL difference of the PCM room roof reached 3.75 °C, 6.5 °C, 25.6% and 70 min, respectively, compared with that of the reference room.
- The east wall showed best thermal performance than the south, north and west walls. The MTR difference, ATFR, DF, and TL difference for this wall in the PCM room reached 2.75 °C, 2.4 °C, 12.8% and 40 min, compared with the reference room.
- Due to extreme hot outdoor weather conditions, the PCM incorporation into building envelope elements was insufficient to maintain an acceptable thermal comfort inside rooms. However, the energy could be saved remarkably during the peak load period. The maximum thermal comfort enhancement in terms of DHR reached a maximum of 11.2% in the period between 10:00 to 11:00.
- The roof, followed by the east wall, showed better MHGR with 11.8% and 9.3%, respectively, which significantly contributed to the energy-saving and thermal comfort inside rooms since they were responsible for 60.6% of the total HG.

5. Study limitations and remarks for future research

The experimental results presented in this study are restricted to the hot climate conditions of the location under study. Same results (with narrow increase/decrease) are expected for hot days during June, July, August and September, the hottest months in southern Iraq.

Using ventilation techniques, preferably by passive means, are recommended to overcome the adverse thermal behaviour of PCM during nighttime. Besides, investigating the night-cooling effect on PCM heat discharging could be investigated in future studies considering the period and time of PCM heat discharging.

CRediT authorship contribution statement

Qudama Al-Yasiri: Conceptualization, Methodology, Data curation, Formal analysis, Investigation, Writing – original draft, Writing – review & editing. **Márta Szabó:** Conceptualization, Formal analysis, Investigation, Writing – review & editing, Supervision, Funding acquisition.

Declaration of Competing Interest

The authors declare that they have no known competing financial interests or personal relationships that could have appeared to influence the work reported in this paper.

Acknowledgements

This work was supported by the Stipendium Hungaricum Scholarship Programme and the Doctoral School of Mechanical Engineering, Hungarian University of Agriculture and Life Sciences, Szent István campus, Gödöllő, Hungary.

References

[1] World Economic Forum. Why buildings are the foundation of an energy-efficient future? 2021. https://www.weforum.org/agenda/2021/02/why-the-buildings-of-the-future-are-key-to-an-efficient-energy-ecosystem/.
[2] Mounir S, Maaloufa Y, Cherki AB, Khabbazi A. Thermal properties of the composite material clay/granular cork. Constr Build Mater 2014;70:183–90.
[3] IEA and UN Environment Programme. 2019 global status report for buildings and construction: Towards a zero-emission, efficient and resilient buildings and construction sector. 2019. https://www.worldgbc.org/news-media/2019-global-status-report-buildings-and-construction.
[4] IEA. Net Zero by 2050: A Roadmap for the Global Energy Sector. 2021. https://www.iea.org/reports/net-zero-by-2050.
[5] Elmokadem A, Shahda M, Elsawaf R. International Journal of Current Engineering and Technology Retrofit an Existing Building Envelope as a Tool to Improve the Energy Performance of Buildings. Int J Curr Eng Technol 2019;9:22–32. https://doi.org/10.14741/ijcet/v.9.1.4.
[6] Piselli C, Castaldo VL, Pisello AL. How to enhance thermal energy storage effect of PCM in roofs with varying solar reflectance: Experimental and numerical assessment of a new roof system for passive cooling in different climate conditions. Sol Energy 2019;192:106–19. https://doi.org/10.1016/j.solener.2018.06.047.
[7] Sadineni SB, Madala S, Boehm RF. Passive building energy savings: A review of building envelope components. Renew Sustain Energy Rev 2011;15:3617–31. https://doi.org/10.1016/j.rser.2011.07.014.

[8] Qi H, Deng J, Li D, Wang F, Arıcı M, Wang Q. Optical properties of paraffin suspension containing TiO2 nanoparticles. Optik (Stuttg) 2020;208:164082. https://doi.org/10.1016/j.ijleo.2019.164082.
[9] Li Y, Chen L. A study on database of modular façade retrofitting building envelope. Energy Build 2020;214:109826. https://doi.org/10.1016/j.enbuild.2020.109826.
[10] Tunçbilek E, Arıcı M, Krajčík M, Nižetić S, Karabay H. Thermal performance based optimization of an office wall containing PCM under intermittent cooling operation. Appl Therm Eng 2020;179:115750. https://doi.org/10.1016/j.applthermaleng.2020.115750.
[11] Li ZX, Al-Rashed AAAA, Rostamzadeh M, Kalbasi R, Shahsavar A, Afrand M. Heat transfer reduction in buildings by embedding phase change material in multi-layer walls: Effects of repositioning, thermophysical properties and thickness of PCM. Energy Convers Manag 2019;195:43–56. https://doi.org/10.1016/j.enconman.2019.04.075.
[12] Li D, Zheng Y, Liu C, Wu G. Numerical analysis on thermal performance of roof contained PCM of a single residential building. Energy Convers Manag 2015;100:147–56. https://doi.org/10.1016/j.enconman.2015.05.014.
[13] Arıcı M, Bilgin F, Nižetić S, Karabay H. PCM integrated to external building walls: An optimization study on maximum activation of latent heat. Appl Therm Eng 2020;165:114560. https://doi.org/10.1016/j.applthermaleng.2019.114560.
[14] Adesina A. Use of phase change materials in concrete: current challenges. Renew Energy Environ Sustain 2019;4:9. https://doi.org/10.1051/rees/2019006.
[15] D'Alessandro A, Pisello AL, Fabiani C, Ubertini F, Cabeza LF, Cotana F. Multifunctional smart concretes with novel phase change materials: Mechanical and thermo-energy investigation. Appl Energy 2018;212:1448–61. https://doi.org/10.1016/j.apenergy.2018.01.014.
[16] Sukontasukkul P, Sutthiphasilp T, Chalodhorn W, Chindaprasirt P. Improving thermal properties of exterior plastering mortars with phase change materials with different melting temperatures: paraffin and polyethylene glycol. Adv Build Energy Res 2019;13(2):220–40. https://doi.org/10.1080/17512549.2018.1488614.
[17] Kheradmand M, Azenha M, de Aguiar JLB, Castro-Gomes J. Experimental and numerical studies of hybrid PCM embedded in plastering mortar for enhanced thermal behaviour of buildings. Energy 2016;94:250–61. https://doi.org/10.1016/j.energy.2015.10.131.
[18] Abden MJ, Tao Z, Pan Z, George L, Wuhrer R. Inclusion of methyl stearate/diatomite composite in gypsum board ceiling for building energy conservation. Appl Energy 2020;259:114113. https://doi.org/10.1016/j.apenergy.2019.114113.
[19] Wang X, Yu H, Li L, Zhao M. Experimental assessment on the use of phase change materials (PCMs)-bricks in the exterior wall of a full-scale room. Energy Convers Manag 2016;120:81–9. https://doi.org/10.1016/j.enconman.2016.04.065.
[20] Memon SA, Cui HZ, Zhang H, Xing F. Utilization of macro encapsulated phase change materials for the development of thermal energy storage and structural lightweight aggregate concrete. Appl Energy 2015;139:43–55. https://doi.org/10.1016/j.apenergy.2014.11.022.
[21] Fateh A, Klinker F, Brütting M, Weinläder H, Devia F. Numerical and experimental investigation of an insulation layer with phase change materials (PCMs). Energy Build 2017;153:231–40. https://doi.org/10.1016/j.enbuild.2017.08.007.
[22] Kośny J. PCM-Enhanced Building Components: An Application of Phase Change Materials in Building Envelopes and Internal Structures. Springer 2015. https://doi.org/10.1007/978-3-319-14286-9.
[23] de Gracia A. Dynamic building envelope with PCM for cooling purposes – Proof of concept. Appl Energy 2019;235:1245–53. https://doi.org/10.1016/j.apenergy.2018.11.061.
[24] Berardi U, Soudian S. Experimental investigation of latent heat thermal energy storage using PCMs with different melting temperatures for building retrofit. Energy Build 2019;185:180–95. https://doi.org/10.1016/j.enbuild.2018.12.016.
[25] Sun X, Zhang Q, Medina MA, Lee KO, Liao S. Parameter design for a phase change material board installed on the inner surface of building exterior envelopes for cooling in China. Energy Convers Manag 2016;120:100–8. https://doi.org/10.1016/j.enconman.2016.04.096.
[26] Mazzeo D, Oliveti G, Arcuri N. Definition of a new set of parameters for the dynamic thermal characterization of PCM layers in the presence of one or more liquid-solid interfaces. Energy Build 2017;141:379–96. https://doi.org/10.1016/j.enbuild.2017.02.027.
[27] Hamdani M, Bekkouche SMEA, Al-Saadi S, Cherier MK, Djeffal R, Zaiani M. Judicious method of integrating phase change materials into a building envelope under Saharan climate. Int J Energy Res 2021;45(12):18048–65. https://doi.org/10.1002/er.6951.
[28] Triano-Juárez J, Macias-Melo EV, Hernández-Pérez I, Aguilar-Castro KM, Xamán J. Thermal behavior of a phase change material in a building roof with and without reflective coating in a warm humid zone. J Build Eng 2020;32:101648. https://doi.org/10.1016/j.jobe.2020.101648.
[29] Wang H, Lu W, Wu Z, Zhang G. Parametric analysis of applying PCM wallboards for energy saving in high-rise lightweight buildings in Shanghai. Renew Energy 2020;145:52–64. https://doi.org/10.1016/j.renene.2019.05.124.
[30] Sovetova M, Memon SA, Kim J. Thermal performance and energy efficiency of building integrated with PCMs in hot desert climate region. Sol Energy 2019;189:357–71. https://doi.org/10.1016/j.solener.2019.07.067.
[31] Louanate A, Otmani RE, Kandoussi K, Boutaous M, Abdelmajid D. Energy saving potential of phase change materials-enhanced building envelope considering the six Moroccan climate zones. J Build Phys 2022;45(4):482–506. https://doi.org/10.1177/17442591211006444.
[32] Bimaganbetova M, Memon SA, Sheriyev A. Performance evaluation of phase change materials suitable for cities representing the whole tropical savanna climate region. Renew Energy 2020;148:402–16. https://doi.org/10.1016/j.renene.2019.10.046.
[33] Sharma V, Rai AC. Performance assessment of residential building envelopes enhanced with phase change materials. Energy Build 2020;208:109664. https://doi.org/10.1016/j.enbuild.2019.109664.
[34] Su W, Darkwa Jo, Kokogiannakis G. Numerical thermal evaluation of laminated binary microencapsulated phase change material drywall systems. Build Simul 2020;13(1):89–98. https://doi.org/10.1007/s12273-019-0563-z.
[35] Lakhdari YA, Chikh S, Campo A. Analysis of the thermal response of a dual phase change material embedded in a multi-layered building envelope. Appl Therm Eng 2020;179:115502. https://doi.org/10.1016/j.applthermaleng.2020.115502.
[36] Rathore PKS, Shukla SK. An experimental evaluation of thermal behavior of the building envelope using macroencapsulated PCM for energy savings. Renew Energy 2020;149:1300–13. https://doi.org/10.1016/j.renene.2019.10.130.
[37] Kenzhekhanov S, Memon SA, Adilkhanova I. Quantitative evaluation of thermal performance and energy saving potential of the building integrated with PCM in a subarctic climate. Energy 2020;192:116607. https://doi.org/10.1016/j.energy.2019.116607.
[38] Ying Kong S, Yang X, Chandra Paul S, Sing Wong L, Šavija B. Thermal Response of Mortar Panels with Different Forms of Macro-Encapsulated Phase Change Materials: A Finite Element Study. Energies 2019;12:2636. https://doi.org/10.3390/en12132636.
[39] Akeiber HJ, Wahid MA, Hussen HM, Mohammad AT. A newly composed paraffin encapsulated prototype roof structure for efficient thermal management in hot climate. Energy 2016;104:99–106. https://doi.org/10.1016/j.energy.2016.03.131.
[40] Saffari M, de Gracia A, Ushak S, Cabeza LF. Passive cooling of buildings with phase change materials using whole-building energy simulation tools: A review. Renew Sustain Energy Rev 2017;80:1239–55. https://doi.org/10.1016/j.rser.2017.05.139.
[41] Köse Murathan E, Manioğlu G. Evaluation of phase change materials used in building components for conservation of energy in buildings in hot dry climatic regions. Renew Energy 2020;162:1919–30. https://doi.org/10.1016/j.renene.2020.09.086.
[42] Costanzo V, Evola G, Marletta L, Nocera F. The effectiveness of phase change materials in relation to summer thermal comfort in air-conditioned office buildings. Build Simul 2018;11(6):1145–61. https://doi.org/10.1007/s12273-018-0468-2.
[43] Al-Yasiri Q, Szabó M. Experimental evaluation of the optimal position of a macroencapsulated phase change material incorporated composite roof under hot climate conditions. Sustain Energy Technol Assessments 2021;45:101121. https://doi.org/10.1016/j.seta.2021.101121.
[44] Al-Yasiri Q, Szabó M. Case study on the optimal thickness of phase change material incorporated composite roof under hot climate conditions. Case Stud Constr Mater 2021;14:e00522. https://doi.org/10.1016/j.cscm.2021.e00522.
[45] Al-Yasiri Q, Szabó M. Thermal performance of concrete bricks based phase change material encapsulated by various aluminium containers: An experimental study under Iraqi hot climate conditions. J Energy Storage 2021;40:102710. https://doi.org/10.1016/j.est.2021.102710.
[46] Al-Yasiri Q, Szabó M. Effect of encapsulation area on the thermal performance of PCM incorporated concrete bricks: A case study under Iraq summer conditions. Case Stud Constr Mater 2021;15:e00686. https://doi.org/10.1016/j.cscm.2021.e00686.
[47] Al-Yasiri Q, Al-Furaiji MA, Alshara AK. Comparative study of building envelope cooling loads in Al-Amarah city. Iraq. J Eng Technol Sci 2019;51(5):632–48. https://doi.org/10.5614/j.eng.technol.sci.2019.51.5.3.
[48] Chaichan MT, Abaas KI, Kazem HA. Design and assessment of solar concentrator distillating system using phase change materials (PCM) suitable for desertic weathers. Desalin Water Treat 2016;57(32):14897–907. https://doi.org/10.1080/19443994.2015.1069221.
[49] Hasan MI. Improving the cooling performance of electrical distribution transformer using transformer oil – Based MEPCM suspension. Eng Sci Technol an Int J 2017;20:502–10. https://doi.org/10.1016/j.jestch.2016.12.003.
[50] Habib NA, Ali AJ, Chaichan MT, Kareem M. Carbon nanotubes/paraffin wax nanocomposite for improving the performance of a solar air heating system. Therm Sci Eng Prog 2021;23:100877. https://doi.org/10.1016/j.tsep.2021.100877.
[51] Chaichan "T, Zaidi MAH, Kazem HA, Sopian K. Photovoltaic Module Electrical Efficiency Enhancement Using Nano Fluids and Nano-Paraffin. IOP Conf. Ser.: Earth Environ. Sci. 2022;961(1):012065. https://doi.org/10.1088/1755-1315/961/1/012065.
[52] Wahid MA, Hosseini SE, Hussen HM, Akeiber HJ, Saud SN, Mohammad AT. An overview of phase change materials for construction architecture thermal management in hot and dry climate region. Appl Therm Eng 2017;112:1240–59. https://doi.org/10.1016/j.applthermaleng.2016.07.032.
[53] Ali AH, Ibrahim SI, Jawad QA, Jawad RS, Chaichan MT. Effect of nanomaterial addition on the thermophysical properties of Iraqi paraffin wax. Case Stud Therm Eng 2019;15:100537. https://doi.org/10.1016/j.csite.2019.100537.
[54] Soliman ARVE-FS. Paraffin as Phase Change Material, Rijeka: IntechOpen; 2020, p. Ch. 5. https://doi.org/10.5772/intechopen.90487.
[55] Ostrý M, Bantová S, Struhala K. Compatibility of Phase Change Materials and Metals: Experimental Evaluation Based on the Corrosion Rate. Molecules 2020;25:2823. https://doi.org/10.3390/molecules25122823.
[56] Salman SA, Shahid S, Ismail T, Chung E-S, Al-Abadi AM. Long-term trends in daily temperature extremes in Iraq. Atmos Res 2017;198:97–107. https://doi.org/10.1016/j.atmosres.2017.08.011.
[57] Ministry of Agriculture, Iraqi Agrometeorological network n.d. http://www.agromet.gov.iq/.

[58] Guarino F, Athienitis A, Cellura M, Bastien D. PCM thermal storage design in buildings: Experimental studies and applications to solaria in cold climates. Appl Energy 2017;185:95–106. https://doi.org/10.1016/j.apenergy.2016.10.046.
[59] Arumugam P, Ramalingam V, Vellaichamy P. Effective PCM, insulation, natural and/or night ventilation techniques to enhance the thermal performance of buildings located in various climates – A review. Energy Build 2022;258:111840. https://doi.org/10.1016/j.enbuild.2022.111840.
[60] de Albuquerque F, Landi F, Fabiani C, Pisello AL. Palm oil for seasonal thermal energy storage applications in buildings: The potential of multiple melting ranges in blends of bio-based fatty acids. J Energy Storage 2020;29. https://doi.org/10.1016/j.est.2020.101431.
[61] Tunçbilek E, Arıcı M, Bouadila S, Wonorahardjo S. Seasonal and annual performance analysis of PCM-integrated building brick under the climatic conditions of Marmara region. J Therm Anal Calorim 2020;141(1):613–24. https://doi.org/10.1007/s10973-020-09320-8.
[62] Sovetova M, Memon SA, Kim J. Energy savings of pcm-incorporated building in hot dry climate. Key Eng Mater 2019;821 KEM:518–24. https://doi.org/10.4028/www.scientific.net/KEM.821.518.
[63] Rathore PKS, Shukla SK, Gupta NK. Yearly analysis of peak temperature, thermal amplitude, time lag and decrement factor of a building envelope in tropical climate. J Build Eng 2020;31:101459. https://doi.org/10.1016/j.jobe.2020.101459.
[64] Hagenau M, Jradi M. Dynamic modeling and performance evaluation of building envelope enhanced with phase change material under Danish conditions. J Energy Storage 2020;30:101536. https://doi.org/10.1016/j.est.2020.101536.
[65] Alam M, Jamil H, Sanjayan J, Wilson J. Energy saving potential of phase change materials in major Australian cities. Energy Build 2014;78:192–201. https://doi.org/10.1016/j.enbuild.2014.04.027.
[66] Nurlybekova G, Memon SA, Adilkhanova I. Quantitative evaluation of the thermal and energy performance of the PCM integrated building in the subtropical climate zone for current and future climate scenario. Energy 2021;219:119587. https://doi.org/10.1016/j.energy.2020.119587.
[67] Thiele AM, Liggett RS, Sant G, Pilon L. Simple thermal evaluation of building envelopes containing phase change materials using a modified admittance method. Energy Build 2017;145:238–50. https://doi.org/10.1016/j.enbuild.2017.03.046.
[68] Asan H. Numerical computation of time lags and decrement factors for different building materials. Build Environ 2006;41:615–20. https://doi.org/10.1016/j.buildenv.2005.02.020.
[69] Jia C, Geng X, Liu F, Gao Y. Thermal behavior improvement of hollow sintered bricks integrated with both thermal insulation material (TIM) and Phase-Change Material (PCM). Case Stud Therm Eng 2021;25:100938. https://doi.org/10.1016/j.csite.2021.100938.
[70] Kontoleon KJ, Stefanidou M, Saboor S, Mazzeo D, Karaoulis A, Zegginis D, et al. Defensive behaviour of building envelopes in terms of mechanical and thermal responsiveness by incorporating PCMs in cement mortar layers. Sustain Energy Technol Assessments 2021;47:101349. https://doi.org/10.1016/j.seta.2021.101349.
[71] Mazzeo D, Kontoleon KJ. The role of inclination and orientation of different building roof typologies on indoor and outdoor environment thermal comfort in Italy and Greece. Sustain Cities Soc 2020;60:102111. https://doi.org/10.1016/j.scs.2020.102111.
[72] Wu Q, Wang J, Meng X. Influence of wall thermal performance on the contribution efficiency of the Phase-Change Material (PCM) layer. Case Stud Therm Eng 2021;28:101398. https://doi.org/10.1016/j.csite.2021.101398.
[73] Zhang Y, Zhuang S, Wang Q, He J. Experimental Research on the Thermal Performance of Composite PCM Hollow Block Walls and Validation of Phase Transition Heat Transfer Models. Adv Mater Sci Eng 2016;2016:1–15. https://doi.org/10.1155/2016/6359414.
[74] Zhang Y, Huang J, Fang X, Ling Z, Zhang Z. Optimal roof structure with multilayer cooling function materials for building energy saving. Int J Energy Res 2020;44(3):1594–606. https://doi.org/10.1002/er.4969.
[75] Imghoure O, Belouaggadia N, Ezzine M, Lbibb R, Younsi Z. Performance evaluation of phase change materials for thermal comfort in a hot climate region. Appl Therm Eng 2021;186:116509. https://doi.org/10.1016/j.applthermaleng.2020.116509.
[76] Vautherot M, Maréchal F, Farid MM. Analysis of energy requirements versus comfort levels for the integration of phase change materials in buildings. J Build Eng 2015;1:53–62. https://doi.org/10.1016/j.jobe.2015.03.003.
[77] ANSI/ASHRAE Standard 55-2010. Thermal environmental conditions for human occupancy. Encycl Financ 2010. https://doi.org/10.1007/0-387-26336-5_1680.
[78] Fanger PO. Thermal comfort: Analysis and applications in environmental engineering. Copenhagen: Danish Technical Press; 1970. https://doi.org/ISBN: 0898744466 9780898744460.
[79] Touma AA, Ouahrani D, Ayas N. Improved Human Thermal Comfort with Indoor PCM-Enhanced Tiles in Living Spaces in the Arabian Gulf. E3S Web Conf 2018;57:04001. https://doi.org/10.1051/e3sconf/20185704001.
[80] Ramakrishnan S, Wang X, Sanjayan J, Wilson J. Thermal performance assessment of phase change material integrated cementitious composites in buildings: Experimental and numerical approach. Appl Energy 2017;207:654–64. https://doi.org/10.1016/j.apenergy.2017.05.144.
[81] Olesen BW, Brager GS. A better way to predict comfort: The new ASHRAE standard 55–2004. ASHRAE J 2004.
[82] Maleki B, Khadang A, Maddah H, Alizadeh M, Kazemian A, Ali HM. Development and thermal performance of nanoencapsulated PCM/ plaster wallboard for thermal energy storage in buildings. J Build Eng 2020;32:101727. https://doi.org/10.1016/j.jobe.2020.101727.
[83] Jamil H, Alam M, Sanjayan J, Wilson J. Investigation of PCM as retrofitting option to enhance occupant thermal comfort in a modern residential building. Energy Build 2016;133:217–29. https://doi.org/10.1016/j.enbuild.2016.09.064.
[84] Ramakrishnan S, Wang X, Sanjayan J, Wilson J. Thermal performance of buildings integrated with phase change materials to reduce heat stress risks during extreme heatwave events. Appl Energy 2017;194:410–21. https://doi.org/10.1016/j.apenergy.2016.04.084.
[85] Sharma A, Sengar N. Heat Gain Study of a Residential Building in Hot-Dry Climatic Zone on Basis of Three Cooling Load Methods. Eur J Eng Res Sci 2019;4:186–94. https://doi.org/10.24018/ejers.2019.4.9.1508.
[86] Lei J, Yang J, Yang E-H. Energy performance of building envelopes integrated with phase change materials for cooling load reduction in tropical Singapore. Appl Energy 2016;162:207–17. https://doi.org/10.1016/j.apenergy.2015.10.031.
[87] Al-Rashed AAAA, Alnaqi AA, Alsarraf J. Energy-saving of building envelope using passive PCM technique: A case study of Kuwait City climate conditions. Sustain Energy Technol Assessments 2021;46:101254. https://doi.org/10.1016/j.seta.2021.101254.
[88] ASHRAE H-F. Chapter 22, Thermal and Moisture Control in Insulated Assemblies—Fundamentals. Am Soc Heating, Refrig Air-Conditioning Eng Inc, Atlanta 1997.
[89] Al-Rashed AAAA, Alnaqi AA, Alsarraf J. Usefulness of loading PCM into envelopes in arid climate based on Köppen-Geiger classification - Annual assessment of energy saving and GHG emission reduction. J Energy Storage 2021;43:103152. https://doi.org/10.1016/j.est.2021.103152.
[90] Fateh A, Borelli D, Devia F, Weinläder H. Summer thermal performances of PCM-integrated insulation layers for light-weight building walls: Effect of orientation and melting point temperature. Therm Sci Eng Prog 2018;6:361–9. https://doi.org/10.1016/j.tsep.2017.12.012.
[91] Kishore RA, Bianchi MVAA, Booten C, Vidal J, Jackson R. Optimizing PCM-Integrated Walls for Potential Energy Savings in US Buildings. Energy Build 2020;226:110355. https://doi.org/10.1016/j.enbuild.2020.110355.
[92] Khdair AI, Abu Rumman G, Basha M. Developing building enhanced with PCM to reduce energy consumption. J Build Eng 2022;48:103923. https://doi.org/10.1016/j.jobe.2021.103923.
[93] Saikia P, Pancholi M, Sood D, Rakshit D. Dynamic optimization of multi-retrofit building envelope for enhanced energy performance with a case study in hot Indian climate. Energy 2020;197:117263. https://doi.org/10.1016/j.energy.2020.117263.
[94] Kumar S, Arun Prakash S, Pandiyarajan V, Geetha NB, Antony Aroul Raj V, Velraj R. Effect of phase change material integration in clay hollow brick composite in building envelope for thermal management of energy efficient buildings. J Build Phys 2020;43(4):351–64. https://doi.org/10.1177/1744259119867462.
[95] Ye R, Lin W, Yuan K, Fang X, Zhang Z. Experimental and numerical investigations on the thermal performance of building plane containing CaCl2·6H2O/expanded graphite composite phase change material. Appl Energy 2017;193:325–35. https://doi.org/10.1016/j.apenergy.2017.02.049.
[96] Hasan MI, Basher HO, Shdhan AO. Experimental investigation of phase change materials for insulation of residential buildings. Sustain Cities Soc 2018;36:42–58. https://doi.org/10.1016/j.scs.2017.10.009.
[97] Akeiber HJ, Hosseini SE, Wahid MA, Hussen HM, Mohammad AT. Phase Change Materials-Assisted Heat Flux Reduction: Experiment and Numerical Analysis. Energies 2016;9:30. https://doi.org/10.3390/en9010030.
[98] Akeiber HJ, Hosseini SE, Hussen HM, Wahid MA, Mohammad AT. Thermal performance and economic evaluation of a newly developed phase change material for effective building encapsulation. Energy Convers Manag 2017;150:48–61. https://doi.org/10.1016/j.enconman.2017.07.043.